UNIVERSITÀ DEGLI STUDI DI VERONA

DEPARTMENT OF

Diagnostic and Public Health

GRADUATE SCHOOL OF

Health and Life Sciences

DOCTORAL PROGRAM IN

Inflammation, Immunity and Cancer

Cycle / year (1° year of attendance) 2015

TITLE OF THE DOCTORAL THESIS

MiT family translocation renal cell carcinoma: looking for diagnostic and druggable markers

S.S.D. MED/08

Coordinator: Prof./ssa Gabriela Costantin

Signature _____

Tutor: Prof. Matteo Brunelli

Signature _____

Doctoral Student: Dott./ssa Anna Caliò

Signature _____

INDEX

SUMMARY

Renal cell carcinomas with chromosome translocation are rare neoplasms which often occur in young patients. In the last World Health Organization (WHO 2016) are named as MiT family translocation renal cell carcinoma comprising two different entities: Xp11 renal cell carcinoma and t(6;11) renal cell carcinoma. Recently, renal cell carcinomas with TFEB amplification has been described in connection with t(6;11) renal cell carcinoma. We analyzed 30 MiT family translocation renal cell carcinoma and 2 renal cell carcinomas with TFEB amplification collecting data on clinical, histological, immunohistochemical and molecular features. In this study, we sought 1) immunohistochemical diagnostic markers (cathepsin K, CD68 (PG-M1), PAX8) since the differential diagnosis is challenging, especially with pure epithelioid PEComa/epithelioid angiomyolipoma; 2) fluorescence in situ hybridization diagnostic features to reach the correct diagnosis; 3) predictive markers (MET, AXL, VEGF) in tumor tissue for target therapy. Histologically, either cytological or architectural appearance was peculiar in each case. By immunohistochemistry, almost all MiT family translocation renal cell carcinomas expressed PAX8. Staining for cathepsin K was found in 65% of Xp11 renal cell carcinomas, only a few cases were positive for melanogenic markers and all cases were negative for CD68 (PG-M1 clone). All t(6;11) renal cell carcinomas labelled for cathepsin K and Melan-A and negative for CD68 (PG-M1 clone). Seven pure epithelioid PEComa /epithelioid angiomyolipomas, used as control, were positive for cathepsin K, melanocytic markers and CD68 (PG-M1) and negative for PAX8. All MiT family translocation renal cell carcinomas were negative for AXL; 61% of Xp11 renal cell carcinomas and 5 of 7 t(6;11) renal cell carcinomas expressed MET. Fluorescence in situ hybridization results showed the presence of *TFEB* gene translocation in all t(6;11) renal cell carcinomas and *TFE3* gene translocation in all Xp11 renal cell carcinoma with a high frequency of split fluorescent signals (mean 74% and 68% respectively). Among the eight t(6;11) renal cell carcinomas, one case displayed a high level of *TFEB* gene amplification and two showed increased *TFEB* gene copy number (3-4 copies of fluorescent signals) with a concomitant increased number of CEP6. Those three cases behaved aggressively. By FISH, *VEGFA* was

amplified in all three cases with *TFEB* amplification and increased VEGFA gene copy number was observed in the two aggressive cases t(6;11) renal cell carcinomas with an overlapping increased number of TFEB fluorescent signals. Overall, VEGFA mRNA expression was observed in 8 of 10 cases (80%); of these 8 cases, three cases showed high level *TFEB* amplification, one case showed *TFEB* rearrangement with increased *TFEB* gene copy number, while four showed *TFEB* gene rearrangement without increased copy number. In conclusion, we report the high frequency of split signals by FISH in MiT family translocation renal cell carcinomas suggesting that 40% of split signals could be used as the proper cut-off to reach the correct diagnosis. We demonstrate the usefulness of CD68 (PG-M1) immunohistochemical staining in distinguishing MiT family translocation renal cell carcinoma from pure epithelioid PEComa/epithelioid angiomyolipoma. Finally, VEGF, MET but not AXL may be potential predictive marker for targeted therapy in MiT family renal cell carcinomas.

INTRODUCTION

The microphthalmia (MiT) family of transcription factors includes four distinctly genes: MITF, TFEB, TFE3, and TFEC. They share sequence homology in their DNA-contacting basic domains and in the transactivation domains. Additionally, these factors can heterodimerize with each other [1]. They physiologically regulate cell growth, differentiation, and survival in several tissue types. Several distinct tumors are associated with the dysregulation of this gene family, including renal cell carcinoma, melanoma, alveolar soft part sarcoma, clear cell sarcoma, and perivascular epithelioid cell neoplasms (PEComas). The new category of MiT family translocation renal cell carcinoma has been included into the World Health Organization(WHO) classification in 2016 [2]. The MiT family renal cell carcinoma comprising two different entities: Xp11 translocation renal cell carcinoma harboring TFE3 gene fusions and t(6;11) renal cell carcinoma harboring a MALAT1-TFEB gene fusion.

Xp11 translocation renal cell carcinoma

Xp11 translocation renal cell carcinomas are a distinctive subtype of renal cell carcinoma characterized by several chromosomal translocations involving TFE3 transcription factor gene. In these tumors, the TFE3 gene is fused by translocation to one of several other genes [3-6]:

- t(X;1) (p11.2; q21.2) gene PRCC
- t (X;17) (p11.2; q25) gene ASPL
- t(X;1) (p11.2; p34) gene SFPQ (PSF)
- t(X;17) (p11.2; q23) gene CLTC
- t(X;3) (p11.2; q21) gene PARP14
- t(X;10) (11.2; q23) unknown gene
- t(X;17) (p11.2; q21.33) gene LUC7L3
- t(X;19) (p11.2; q13.3) gene KHSRP
- t(X;17) (p11.2; p13) gene DVL2
- t(X;22) (p11.2; q11.21) gene MED15
- t(X;6) (p11.2; q25.3) gene ARIDB
- t(X;5) (p11.2; q31.2) gene MATR3

- t(X;1) (p11.2; p31.1) gene FUBP1
- inv (X) (p11.2; q12) gene NONO (p54*nrb*)
- inv(X) (p11.2; p11.3) gene RBM10
- inv(X)(p11.23;p11.23) il gene GRIPAP1

The three most common Xp11 translocation renal cell carcinomas are those bearing the t(X;1)(p11.2;q21) which fuses the PRCC and TFE3 genes, the t(X;17)(p11.2;q25) which fuses the ASPL and TFE3 genes, and the t(X;1)(p11.2;p34) which fuses the SFPQ (PSF) and TFE3 genes. Of interest, either t(X;17) renal cell carcinoma or alveolar soft part sarcoma harbor the same ASPL-TFE3 fusion gene [7]. However, the translocation is balanced in t(X;17) renal cell carcinoma and unbalanced in alveolar soft part sarcoma, which may contribute to the clinical and morphological differences. The function of chimeric TFE3 fusion proteins can also vary which may explain the different histologic features observed in this tumor entity of renal cell carcinoma.

Clinical Features

Xp11 renal cell carcinoma comprises 20–75% of childhood renal cell carcinoma and 1–4% of adult renal cell carcinoma with an average age of onset of 50 years [8] .The incidence of Xp11 translocation renal cell carcinoma in adults may be underestimated, likely for the morphological overlap with more common adult renal cell carcinoma subtypes, such as clear cell and papillary renal cell carcinoma. Clinically, there is not a typical presenting features. As is common for other renal cell carcinomas, roughly one-third of tumors is asymptomatic, often accidentally discovered. Prior exposure to cytotoxic chemotherapy has been reported as a risk factor [9].

Pathologic Features

Gross Findings

There is no a specific macroscopic appearance of Xp11 translocation renal cell carcinoma. They usually present as solitary cortical masses characterized by

tan-yellow cut surfaces with foci of hemorrhage and necrosis and occasionally focal cystic degeneration.

Microscopic Features

Histologically, Xp11 translocation renal cell carcinomas are characterized by heterogeneous architectural and cytologic features mimicking almost all subtypes of renal cell carcinoma. The most distinctive histologic pattern is the presence of papillary architecture with epithelioid clear cells. However, different architectures have been reported such as solid, nested, trabecular, and microcystic pattern. Tumor cells are clear to eosinophilic with varying amounts of cytoplasm. The nuclei may show variability in size and are generally large with a prominent eosinophilic nucleoli (typically G3 by ISUP/WHO 2016). Psammoma bodies are often present. The wide spectrum of morphology reported in Xp11 translocation renal cell carcinomas emphasizes the need to consider these carcinomas in the differential diagnosis of unusual renal cell carcinomas occurring in both children and adults [3].

Immunohistochemical features

Like other subtypes of renal cell carcinoma, Xp11 translocation renal cell carcinoma are positive for PAX8. Vimentin and CK7 are typically negative. Staining for CD10 is generally reported. Occasionally, Xp11 translocation renal cell carcinoma may express melanogenic markers such as Melan-A and HMB45. Cathepsin K is overexpressed in a subset of Xp11 translocation renal cell carcinomas (approximately 60%). Interestingly, PRCC-TFE3 renal cell carcinoma is labelled more frequently for cathepsin K than ASPL-TFE3 renal cell carcinoma [10, 11]. TFE3 immunostaining, initially considered as the most sensitive and specific marker, should be cautiously used due to the not infrequent false-positive and false negative results [12]. For this reason, the identification of the TFE3 rearrangement by FISH assays on formalin-fixed and paraffin-embedded tissue sections is currently the gold standard to reach the correct diagnosis [12].

Prognosis and Treatment

The outcome of Xp11 translocation renal cell carcinoma is highly variable, with some patients surviving decades with indolent disease and others dying rapidly of progressive disease. Overall, Xp11 translocation renal cell carcinoma shows lymph node metastasis and has a worse prognosis than papillary renal cell carcinoma and similar prognosis with clear cell renal cell carcinoma [13]. Several studies have demonstrated that Xp11 translocation renal cell carcinoma in children have a relatively indolent course, despite their often advanced stage at presentation. Among Xp11 translocation renal cell carcinoma, patients with ASPL-TFE3 fusion have a worse prognosis, but it is still unclear whether the fusion partner plays a prognostic role [13, 14].

The optimal therapy for the Xp11 translocation renal cell carcinoma remains to be determined. For localized tumors, including patients with positive regional lymph nodes, surgery is the treatment of choice. For patients with hematogenous metastases, the current options are immunotherapy, therapies targeting vascular endothelial growth factor receptor, and target therapies for MET signaling pathway [15-18]. Unfortunately, to date there is no data regarding predictive markers to choose the best therapy for the single patient.

t(6;11) renal cell carcinoma

T (6;11) renal cell carcinoma is an extremely rare variant and accounts for 0.02% of all renal carcinomas. Although the initial description was in children [19], t(6,11) renal cell carcinoma may occur in adults in the age range of other renal cell carcinomas. The t(6;11) translocation fuses the gene for TFEB with Alpha (MALAT1), an untranslated gene of unknown function, resulting in overexpression of native TFEB.

Clinical Features

The t(6;11) renal cell carcinomas are less common than the Xp11 renal cell carcinomas; approximately 60 cases documented in the literature, the majority of which in children and adolescents. However, it has been demonstrated that these neoplasms can occur in adults as well. The mean age of presentation is 34 years,

with a wide reported range of 3-77years. The tumor is usually an incidental finding. Similar to Xp11 translocation renal cell carcinoma, a subset of cases has occurred in patients who have received cytotoxic chemotherapy for other reasons.

Pathologic Features

Gross Findings

As Xp11 translocation renal cell carcinoma, t(6;11) renal cell carcinoma does not have a distinctive gross appearance.

Microscopic Features

Histologically, t(6;11) renal cell carcinoma has been classically characterized by a distinctive biphasic morphology with larger epithelioid cells and smaller cells clustered around eosinophilic spheres formed by basement membrane material [3]. However, several reports have shown a broad range of morphology in molecular confirmed t(6;11) renal cell carcinomas. Papillary and tubulocystic architectures, clear cell and oncocytoma-like features, diffuse hyalinization with thick-walled blood vessels are some of the unusual pathological features described [3]. The wide spectrum of morphology results in several differential diagnoses including Xp11 translocation renal cell carcinoma, pure epithelioid PEComa /epithelioid angiomyolipoma, and other more common types of renal cell carcinoma [20-22]. Among them, pure epithelioid PEComa /epithelioid angiomyolipoma is the most challenging.

Immunohistochemical features

Immunohistochemically, most t(6;11) renal cell carcinomas express PAX8, supporting renal tubular differentiation and melanogenic markers, such as HMB-45 and Melan-A. Cathepsin K is overexpressed in almost all t(6;11) renal cell carcinomas[23, 24]. Staining for TFEB was considered highly sensitive and specific for this tumor. However, the results can be inconsistent among laboratories, mainly because of technical factors such as fixation time and differences in the methods of antigen retrieval. Like Xp11 translocation renal cell

carcinomas, the identification of the rearrangement by FISH analysis is the gold standard for the diagnosis [25].

Prognosis and Treatment

Most instances of t(6;11) renal cell carcinoma have an indolent clinical course with a few published cases demonstrating aggressive behavior [3]. There are no well-established prognostic markers to predict the biological behavior.

The radical surgery remains the best therapeutic strategy. Because of the rarity of this tumor, no information regarding neoadjuvant or adjuvant therapies are available. Like Xp11 renal cell carcinoma, these neoplasms have demonstrated the capacity to recur late (up to 8 years after diagnosis), so long-term follow-up is important for these patients.

Renal cell carcinoma with TFEB amplification

More recently, renal cell carcinomas with TFEB amplification have been identified and appear to be associated with a more aggressive clinical course.

TFEB amplification in renal cell carcinoma can occur independently of or in association with *TFEB* rearrangement. *TFEB* gene rearrangement via chromosome translocation or amplification causes intact TFEB overexpression and drives subsequent expression of immunohistochemical markers such as cathepsin K, Melan-A and HMB45 [23]. However, TFEB amplified renal cell carcinomas differ from TFEB-translocation renal cell carcinomas in several ways [26]. First, they typically occur in older patients (mean 65 years) compared to unamplified TFEB translocation RCC (mean age 31 years). Second, their morphology is usually high grade and less distinctive than the biphasic appearance of the typical TFEB-translocation renal cell carcinoma. Third, melanogenic marker expression is less consistent: while all cases have expressed Melan-A, only approximately 50% express cathepsin K and HMB45. Fourth, TFEB amplified renal cell carcinomas typically have an aggressive clinical course while TFEB-translocation renal cell carcinoma usually are indolent.

TFEB gene is located in the short arm of chromosome 6, specifically in the 6p21-p23 region, immediately adjacent to vascular endothelial growth factor A

(*VEGFA*) gene. Given the proximity of those two genes, it has been hypothesized and demonstrated that some renal cell carcinomas showing *TFEB* amplification harbor concurrent *VEGFA* amplification [27].

MATERIAL AND METHODS

Patients and samples

Thirty MiT family translocation renal cell carcinomas and 2 TFEB-amplified real cell carcinomas were retrieved from the files of University of Verona. The number of blocks from which hematoxylin eosin-stained sections were available for each tumor ranged from 1 to 41 (median 8). All slides were reviewed by two expert pathologists (AC, GM). For each case the following morphologic features were recorded: solid, nested, tubulocystic and papillary architecture, the presence of pseudocapsule, hyalinized stroma, necrosis and psammoma bodies. With respect to cellular features, the presence of small cells around the basement membrane, eosinophilic and clear cytoplasm, nucleolar grade according to ISUP/WHO 2016, and mitotic figures were assessed.

Immunohistochemistry

Sections from tissue blocks of MiT family translocation renal cell carcinomas and TFEB amplified renal cell carcinomas were immunohistochemically stained with the following antibodies: PAX8 (clone BC12, DSB), Cathepsin K (clone 3F9, dilution 1:2000, Abcam), HMB45 (dilution 1:30, Dako), Melan-A (clone A103, dilution 1:50, Novocastra), CD68 (clone PG-M1, dilution 1:50, Dako and clone KP1, dilution 1:400, Dako) and cytokeratin 8-18 (clone 5D3, dilution 1:100, Novocastra). To evaluate the possible predictive markers in tumor tissue, all 30 MiT family translocation renal cell carcinomas were immunohistochemically stained with MET (clone SP44, prediluted, Ventana), AXL (clone C89E7, dilution 1:100, Cell Signallig). Seven pure epithelioid PEComa /epithelioid angiomyolipomas were immunohistochemically labeled with the same panel for comparison. All samples were processed using a sensitive “Bond Polymer Refine” detection system in an automated Bond

immunohistochemistry instrument (Leica Biosystems). The appropriate positive and negative controls were concurrently carried out. Labeling for each marker was recorded as the percentage of positive cells. With regards on the results of MET immunostaining, a grading of the intensity was also recorded by using a scoring scale based on three values: + (mild), ++ (intermediate) and +++ (strong).

Fluorescence *in situ* hybridization (FISH)

Fluorescence in situ hybridization (FISH) was carried out on the 32 tumors and the 37 control cases (10 clear cell renal cell carcinomas, 10 papillary renal cell carcinomas, 5 chromophobe renal cell carcinomas, 5 oncocytomas and 7 pure epithelioid PEComa /epithelioid angiomyolipomas) using dual color break apart TFE3 and TFEB probe (Cytotest Inc, Rockville, MD 20850, USA) and VEGFA (ZytoVision, Bremerhaven, Germany) probe. Centromeric alpha-satellite specific for chromosome 6 (CEP6) was used as control probes (Vysis-Abbott, Olympus, Rome, Italy) on serial tissue sections. Briefly, 3 µm sections were cut from formalin-fixed paraffin-embedded tissue blocks and mounted on positively charged slides. The slides were dried for one hour at 60°C then deparaffinized, rehydrated and fixed in methanol/acetic acid 3:1 for 5 min. Pretreatment was performed at 85°C for 30 min with 0,1 citrate buffer (pH6) solution followed by pepsin (4mg./ml in 0.9% NaCl, pH 1,5) treatment for 8 min at 37°C. After washing and dehydration, 10 µl probe was applied on selected area and sealed with rubber cement. Denaturation was assessed by incubating the slides at 80°C for 10 min in a humidified atmosphere (Thermobrite System) followed by hybridization overnight at 37°C. The rubber cement and the cover slip were removed and the slides were washed in 2X SSC/0,3% NP40 for 15 min at room temperature and then at 72°C for 2 min. Next, the tissue sections were counterstained with DAPI antifade (Prolong Gold Antifade Reagent Life Technologies) and examined under an X60- X100 oil immersion objective using an Olympus BX61 fluorescence microscope equipped with filters that visualize the different wavelengths of the fluorescent probe.

Scoring was performed by two experienced pathologists (AC and MB). At least 100 neoplastic non-overlapping nuclei were included in the scoring. To

avoid false positive results due to nuclear truncation, cells with a single fluorescent signal were not evaluated. Ratio between mean copy number of *TFEB* gene / mean copy number of control centromeric probes CEP6 was ultimately scored. Amplification was defined by the presence of >10 TFEB/VEGFA fluorescent signals or the LSI/CEP ratio was ≥2.

mRNA *in situ* hybridization (RNAscope)

The samples were analyzed with RNAscope assay (Advanced Cell Diagnostics, Newark CA USA) using RNAscope 2.5 HD Assay-Brown kit and the Probes-Hs-VEGFA. Ten renal tumors (3 clear cell renal cell carcinomas, 3 papillary renal cell carcinomas, 2 chromophobe renal cell carcinomas, 2 oncocytomas) were used as control cases. The procedure was performed manually following the manufacturer's instructions. We used freshly cut 3µm. formalin-fixed and paraffin-embedded slides dried for 1h at 60°C. The sections were deparaffinized and treated with the peroxidase block solution for 10 minutes at room temperature and then with retrieval solution for 15 minutes at 99°C. For each case 3 sections with targeted probes were incubated: VEGFA, DAPB as negative control and UBC as positive control. The hybridization was performed for 2 h at 40°C. Slides were then washed and incubated with the signal amplification solution: amp1 for 30 minutes at 40°C, amp2 for 15 minutes at 40°C, amp3 for 30 minutes at 40°C, amp4 for 15 minutes at 40°C, amp5 for 30 minutes at room temperature, amp6 for 15 minutes at room temperature and finally with DAB for 10 minutes and hematoxylin for the counterstaining. The results were examined under a standard bright-field microscope at X60 magnification. Scoring was performed according to ACD guideline for semi-quantitative assessment of RNAscope staining intensity as (0,1,2,3,4) (https://acdbio.com/technical-support/solutions). A positive result was considered when the neoplastic cells showed 3 or 4 intensity staining.

Cytogenetic analysis

Cells were cultured with in situ method (cover glass in a 35mm petri dish) and RPMI 1640 medium 20% FBS and harvested following standard cytogenetic

techniques. Briefly, each dish was examined daily after the fourth day for growth and the rate of proliferation. When cultures were ready the cells were exposed to colcemid (0.01 mg/ml) for 15 hours (overnight), hypotonic treatment (0.1% sodium citrate) and fixative solution (Carnoy). Karyotype was studied in QFQ banding (quinacrine dihydrochloride 500mg/100ml) by fluorescence microscopy. FISH was performed using TUPLE1 probe (Cytocell) following the manufacturer protocol.

Statistical analysis

Fisher's exact test was used to compare categorical data for clinical and pathological characteristics and Student's t test to compare continuous data. All *P* values are based on a two-tailed hypothesis. The results were considered statistically significant if the *P* value was less than 0.05.

RESULTS

The results for Xp11 renal cell carcinomas and t(6;11) renal cell carcinomas were separately described for simplicity.

Xp11 renal cell carcinoma

Clinical features

The clinical charateristics are detailed in Table 1. Eleven patients were females and nine males (F:M ratio, 1:1,2). The patients' ages at diagnosis ranged from 10 to 75 years (mean 39, median 38). Patient 19 had a solid pseudopapillary tumor of the pancreas and the renal mass was an incidental finding. Follow up was available for thirteen patients, ranging from 6 to 132 months (mean 52, median 33). Three patients (patient 9, 13 and 16) were metastatic at the time of the diagnosis while one patient (patient 7) developed multiple peritoneal metastasis after 60 months from radical nephrectomy. Patient 16 began sunitinib for roughly one year with slight shrinkage of the renal mass. Because the remarkable progression on the liver metastases, nivolumab was initiated.

However, due to the frank progression on liver and bone metastases, the treatment was changed after two months. He received cabozantinib and died after two weeks from the beginning of the third line of treatment. Patient 13 is currently receiving sunitinib, and he is alive 4 months after the diagnosis with liver metastasis.

Table 1. Clinical and pathological features of Xp11 renal cell carcinomas

Case	Age	Gender	Size/laterality	Stage TNM	Surgery	Follow-up
1	33	F	n.a.	n.a.	n.a.	84 months alive
2	75	F	4 cm/L	pT1aNxMx	Radical nephrectomy	24 months alive
3	26	F	3 cm/n.a.	pT1aNxMx	Partial nephrectomy	12 months alive
4	43	M	7 cm/L	pT1bN1Mx	Radical nephrectomy	lymphnodes metastasis
5	56	M	6,6 cm/R	pT3aNxMx	Radical nephrectomy	n.a.
6	31	M	10 cm/L	pT2aNxMx	Radical nephrectomy	n.a.
7	27	M	n.a./R	n.a.	Radical nephrectomy	multiple peritoneal metastasis after 60 months
8	29	M	n.a.	n.a.	n.a.	n.a.
9	43	F	1cm/L	pT1aN1M1	Partial nephrectomy	60 months alive with supravicular lymph node metastasis
10	70	F	7 cm/L	pT1bNxMx	n.a.	120 months alive
11	39	F	6 cm/L	pT1bN0M0	Radical nephrectomy	6 months alive
12	n.a.	n.a.	n.a.	n.a.	n.a.	n.a.
13	65	M	n.a./R	pT4N1M1	Not performed	4 months alive with multiple hepatic metastasis
14	16	M	n.a./L	n.a.	n.a.	120 months alive
15	10	F	n.a./R	n.a.	Radical nephrectomy	132 months alive
16	25	M	6 cm/L	pT1bN1M1	Not performed	dead after 17 months with bone, liver, abdominal and mediastinal lymph nodes metastases
17	43	F	6,6 cm/L	pT1bNxMx	n.a.	33 months alive
18	54	F	2,8 cm/L	pT1aNxMx	n.a.	n.a.
19	31	F	1,3 cm/R	pT1aNxMx	Partial nephrectomy	6 months alive
20	n.a.	n.a.	n.a.	n.a.	n.a.	n.a.
21	37	M	3,5 cm/R	pT1aNxMx	n.a.	n.a.
22	67	F	2,5 cm/R	pT1aNxMx	Partial nephrectomy	n.a.

F: female, M: male, R: right, L: left, n.a.: not available

Pathological features

Twenty samples derived from the resection of the primary tumor (either radical or partial nephrectomy) two samples derived from lymph node metastasis (case 9) and renal biopsy (case 13) respectively. The tumors ranged in size from 1.3 to 10 cm (mean 5, median 6). The tumors were mainly solid with three cases multicystic. The morphological features are summarized in Table 2. The architectural patterns observed were papillary, tubular, cystic, alveolar, glandular, solid and nested, usually in combination. Necrosis was detected in 24% of the tumors, calcifications in 57%, and the presence of an incomplete pseudocapsule in 43%. The tumor cells ranged in size from small to large with clear to granular eosinophilic cytoplasm. A biphasic architecture resembling the morphology of t(6;11) renal cell carcinoma was observed in one neoplasm (case 8). The most common nucleolar grade observed was G2 (48%), and G3 (48%) and only one case had a G1 score (4%) by ISUP/WHO 2016.

Case 1

The tumor showed pushing margins and made up of clear and eosinophilic polygonal cells with conspicuous nucleoli (G2 by ISUP/WHO 2016) arranged in solid/alveolar and psudopapillary architecture. Areas of hyalinized stroma, psammoma bodies, hemorrhagic areas and pigment bearing histiocytes were found (Figure 1f). No necrosis was observed.

Case 2 and Case 3

The tumor was multicystic lined by a single layer of cells showing abundant vacuolated clear cytoplasm with round nuclei and pinpoint nucleoli (G2 by ISUP/WHO 2016). Psammoma bodies were extensively present. Necrosis was absent.

Case 4

A discontinuous pseudocapsule was present. The neoplasm was mainly composed of large polygonal cells with well-defined cell borders, eosinophilic cytoplasm and central round nuclei with prominent nucleoli (G3 by ISUP/WHO 2016) arranged in solid/alveolar and tubular-papillary architecture. Lymphovascular invasion, peritumoral inflammatory cells and a few psamomma

bodies were seen. Focal necrosis was present. Five of seven hilar lymph nodes examined were positive for tumor metastasis.

Case 5

The tumor was characterized by cells with clear to eosinophilic cytoplasm and small nuclei (G2 by ISUP/WHO 2016) arranged in papillary architecture and solid-alveolar pattern. A few psammoma bodies were found.

Case 6

The neoplasm was mainly composed of nests of polygonal cells with clear cytoplasm and central round nuclei with prominent nucleoli (G3 by ISUP/WHO 2016) separated by thick fibrous tissue bundles. Additional areas showing cells with granular and eosinophilic cytoplasm were present. Tubular and papillary structures were also observed. Psammoma bodies and pigment bearing histiocytes were encountered. No necrosis was found.

Case 7

A discontinuous pseudocapsule was present. The neoplasm was mainly composed of cells with abundant eosinophilic cytoplasm and central round nuclei with prominent nucleoli (G3 by ISUP/WHO 2016) arranged in a solid alveolar pattern. Necrosis was present.

Case 8

The tumor was partially made up of granular eosinophilic polygonal cells with conspicuous nucleoli (G2 by ISUP/WHO 2016) arranged in solid and tubular/alveolar architecture. At low power magnification, a biphasic population resembling the morphology of t(6;11) renal cell carcinoma were easily observed (Figure 2). At the periphery of the tumor, entrapped renal normal tubules were focally present.

Case 9

Surgical sample of lymph node metastasis was available for histological characterization and consisted of clear cells with distinct borders and small round nuclei (G2 by ISUP/WHO 2016) (Figure 2) with several psammoma bodies.

Case 10

The tumor was multicystic lined by a single layer of cells showing abundant vacuolated clear cytoplasm with round nuclei and pinpoint nucleoli (G1

by ISUP/WHO 2016) (Figure 1). Psammoma bodies were extensively present. Necrosis was absent.

Case 11

A discontinuous thick pseudocapsule was present. The tumor was composed of epithelioid cells with eosinophilic and focally clear cytoplasm and prominent nucleoli (G3 by ISUP/WHO 2016) mainly arranged in solid-tubular architecture. Neoplastic lymphovascular invasion and extensive necrosis were seen. Neither perirenal adipose tissue invasion nor renal sinus invasion was found.

Case 12

The tumor was well-delineated by a pseudocapsule. At low power magnification, papillary architecture made up of small cells with eosinophilic cytoplasm and round hypercromic nuclei (G2 by ISUP/WHO 2016) was observed. Additional areas mainly composed of clear cells with nuclear inclusions arranged in a solid-alveolar pattern were present (G2 by ISUP/WHO 2016). Several psammoma bodies were found throughout the tumor.

Case 13

The biopsy showed an epithelial neoplasm made up of sheets of small cells with round nuclei (G2 by ISUP/WHO 2016) and eosinophilic cytoplasm arranged in tubule-papillary architecture (Figure 2). No necrosis was observed.

Case 14

A fibrous thick pseudocapsule with dystrophic calcification was present (Figure 1). The tumor was composed of epithelioid cells with clear cytoplasm and small nucleoli (G2 by ISUP/WHO 2016) mainly arranged in solid and papillary architecture. Areas with granular eosinophilic cells with prominent nucleoli (G3 by ISUP/WHO 2016) were observed. Hyaline sclerosis was seen.

Case 15

The tumor was characterized by cells with eosinophilic cytoplasm and small nuclei (G2 by ISUP/WHO 2016) arranged in papillary pattern with psammoma bodies.

Case 16

The tumor was solid and focal papillary composed of large epithelioid cells with eosinophilic to focally clear cytoplasm with prominent nucleoli (G3 by ISUP/WHO 2016). Areas of extensive tumoral necrosis was observed.

Case 17

A discontinuous thick pseudocapsule was present. The tumor was composed of epithelioid cells with clear cytoplasm and small nucleoli (G2 by ISUP/WHO 2016) mainly arranged in solid-alveolar architecture. Areas with microcystic pattern and aggregates of histiocytes were seen. No necrosis was found.

Case 18

A discontinuous thin pseudocapsule was present. The neoplasm was mainly composed of polygonal cells with eosinophilic to focally clear cytoplasm and central round nuclei with prominent nucleoli (G3 by ISUP/WHO 2016) arranged in a papillary architecture. Focally necrosis was encountered.

Case 19

The tumor showed a papillary architecture (Figure 1). The neoplastic cells were large and epithelioid with abundant clear cytoplasm and enlarged hyperchromatic nucleoli (G3 by ISUP/WHO 2016) (Figure 2). Histiocytes and psammoma bodies were present.

Case 20: No information available.

Case 21

The tumor was well-delineated by a pseudocapsule. However, an infiltrative growth of the neoplastic cells through the pseudocapsule was frequently observed. At low power magnification, a mixture of tubular, papillary and microcystic patterns was seen. The neoplastic cells showed a clear cytoplasm and enlarged nucleoli (G3 by ISUP/WHO 2016). Several psammoma bodies were found. Necrosis was absent.

Case 22

A discontinuous pseudocapsule was present. The tumor consisted of clear to focally eosinophilic cells with prominent nucleoli (G3 by ISUP/WHO 2016). Architecturally, tubular-glandular areas and papillary changes were observed.

No necrosis was observed.

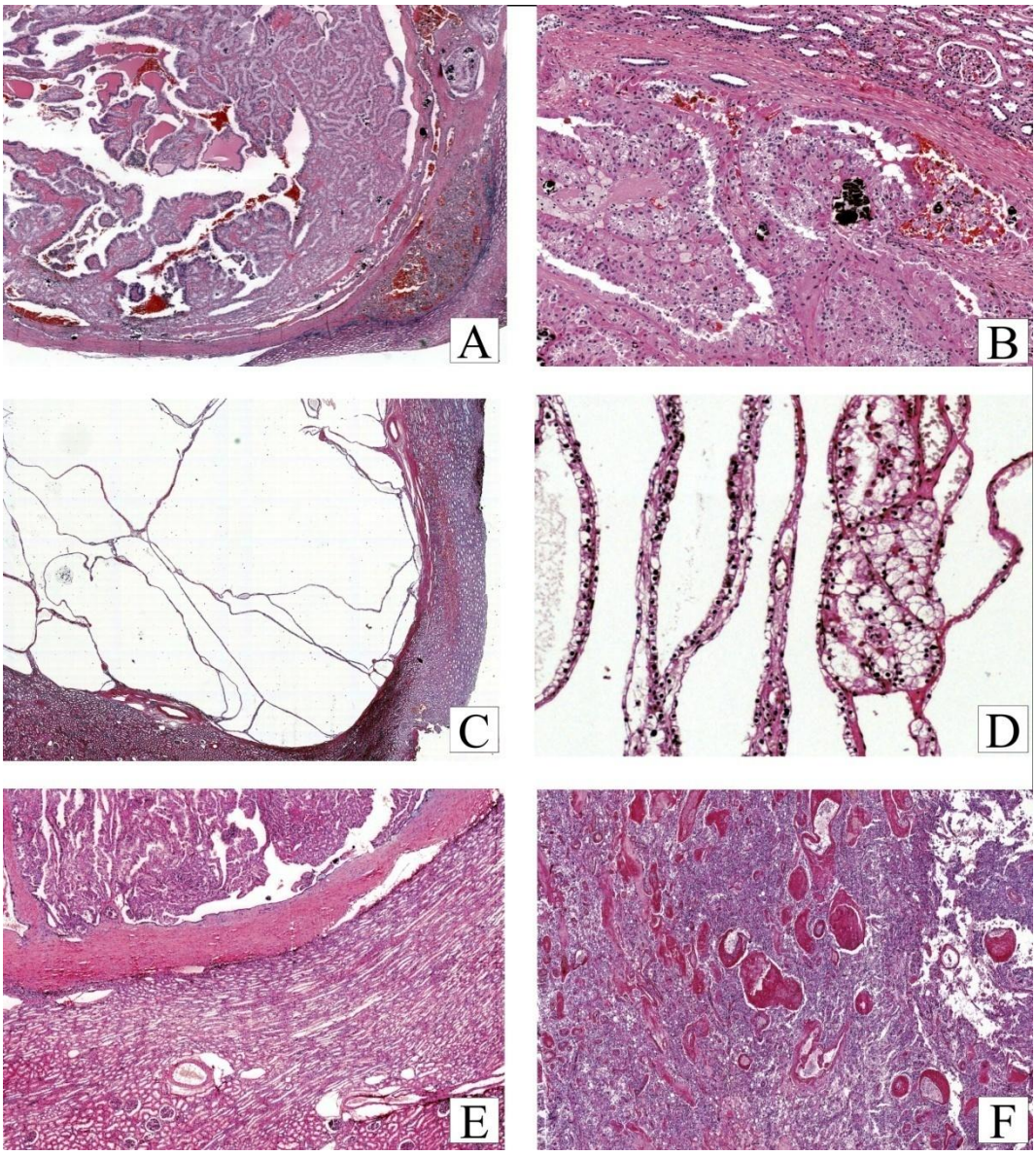

Figure 1. Different histologic appearances of Xp11 renal cell carcinoma.
Neoplasm with papillary/tubular architecture composed by eosinophilic epithelioid cells (A, B) with psammoma bodies (B). A multicystic tumor (C) lined by clear cells (D). The presence of a thick pseudocapsule is a common feature (E). Hyaline sclerosis may be observed (F).

Table 2 . Histological features of Xp11 renal cell carcinoma

Case	Architecture	Cellular features: size/staining	ISUP grade	Necrosis
1	pseudopapillary/solid	medium / clear and eosinophilic	G2	absent
2	multicystic	medium / clear	G2	absent
3	multicystic	medium / clear	G2	absent
4	solid-alveolar/papillary	large / eosinophilic	G3	present
5	solid-alveolar/papillary	medium / clear and eosinophilic	G2	absent
6	nested/tubular-papillary	medium / clear and eosinophilic	G3	absent
7	solid-alveolar	large / eosinophilic	G3	present
8	biphasic: solid / tubular	medium / eosinophilic	G2	absent
9	solid-alveolar	medium / clear	G2	absent
10	multicystic	medium / clear	G1	absent
11	solid/tubular	large / eosinophilic	G3	present
12	solid-alveolar/papillary	small / eosinophilic - medium / clear	G2	absent
13	papillary	small / eosinophilic	G2	absent
14	solid-alveolar/papillary	medium / clear and eosinophilic	G3	absent
15	papillary	small / eosinophilic	G2	absent
16	solid/papillary	medium / clear and eosinophilic	G3	present
17	solid-alveolar/microcystic	medium / clear	G2	absent
18	papillary	medium / clear and eosinophilic	G3	present
19	papillary	medium / clear and eosinophilic	G3	absent
20	n.a.	n.a.	n.a	n.a
21	tubular/papillary/microcystic	medium / clear and eosinophilic	G3	absent
22	tubular/papillary	medium / clear and eosinophilic	G3	absent

n.a.: not available

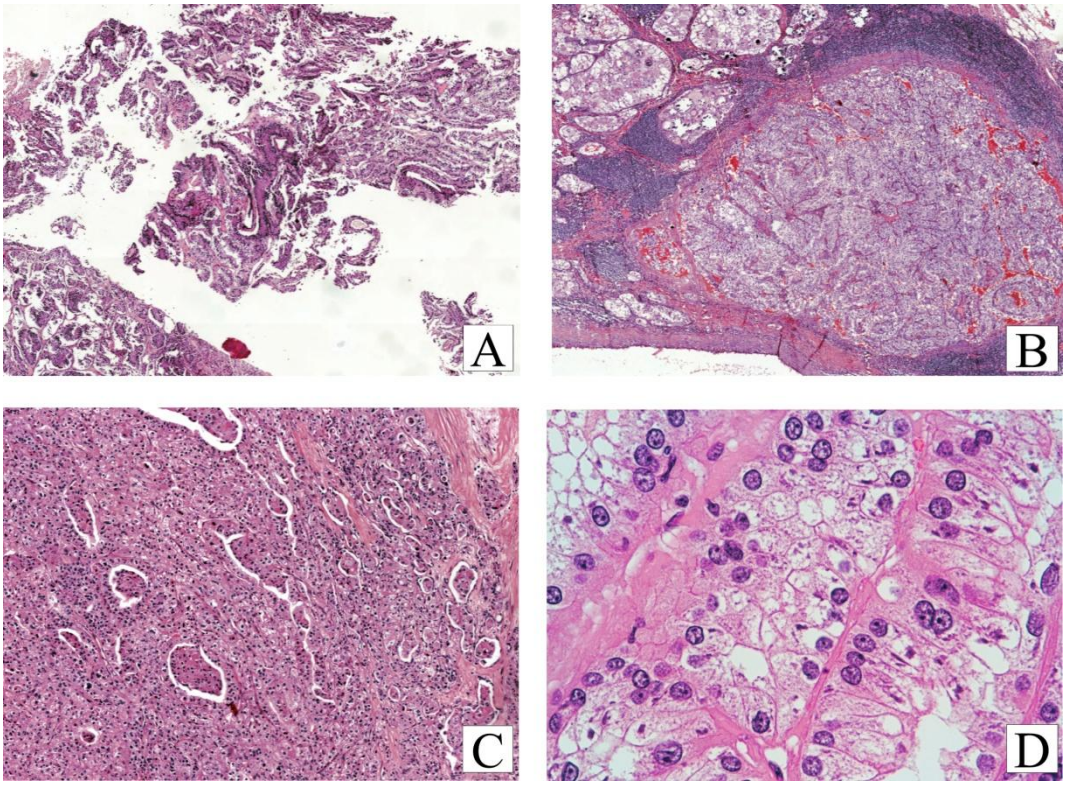

Figure 2. Different histologic appearances of Xp11 renal cell carcinoma.
Biopsy sample showing tubular/papillary tumor composed by small eosinophilic cells (A). Lymph node metastasis of epithelial tumor with alveolar architecture made up of clear and eosinophilic cells (B). At low power magnification, a biphasic population resembling the morphology of t(6;11) renal cell carcinoma were easily observed (C). At high magnification, prominent nucleoli is a common characteristic (D).

Immunohistochemical features

The immunohistochemical results are reported in Table 3. Almost all cases (89%) were positive for PAX8 with a percentage of positive cells ranging from 5% to 100%. Staining for cathepsin K was observed in thirteen of twenty tumors (65%). Among those, five tumors were positive for HMB45 with a percentage of positive cells ranging from 5% to 100%; whereas all cathepsin K negative tumors were also negative for HMB45 . The three multicystic tumors were the only cases immunolabeled for Melan-A. Eleven of eighteen tumors (61%) were positive for MET with a percentage of positive cells that ranged from 1% to 100%. All the tumors examined were negative for CD68 (PG-M1) and AXL.

Table 3. Immunohistochemical features of Xp11 renal cell carcinoma

Case	PAX 8	Cathepsin K	HMB45	MelanA	CD68(PG-M1)	MET	AXL
1	5%+	80%+	15%+	neg	neg	10% ++	neg
2	80%+	100% +	neg	70%+	neg	10% +	neg
3	90%+	100% +	neg	80%+	neg	70% ++	neg
4	5%+	100% +	neg	neg	neg	30%++ / 20%+	neg
5	n.a.	90% +	neg	n.a.	n.a.	neg	neg
6	neg	100% +	100% +	neg	n.a.	1% +	neg
7	neg	90% +	neg	neg	neg	neg	neg
8	5%+	100% +	5%+	neg	neg	5% +	neg
9	100%+	100% +	neg	neg	neg	100% ++	neg
10	100%+	100% +	neg	10%+	neg	neg	neg
11	70% +	90% +	89% +	neg	neg	10% ++	neg
12	60%+	30% +	5% +	neg	neg	neg	neg
13	90% +	80% +	neg	neg	n.a.	n.a.	neg
14	10%+	neg	neg	neg	neg	5% +	neg
15	50%+	neg	neg	neg	neg	neg	neg
16	90 % +	neg	n.a.	n.a.	neg	n.a.	neg
17	n.a.	neg	neg	n.a.	n.a.	n.a.	neg
18	100% +	neg	neg	neg	n.a.	neg	neg
19	100% +	neg	neg	neg	neg	50% ++ / 30%+	neg
20	n.a.	n.a.	n.a.	n.a.	n.a.	n.a.	neg
21	n.a.	n.a.	n.a.	n.a.	n.a.	neg	neg
22	90% +	neg	n.a.	n.a.	n.a.	100% +++	neg

n.a.: not available

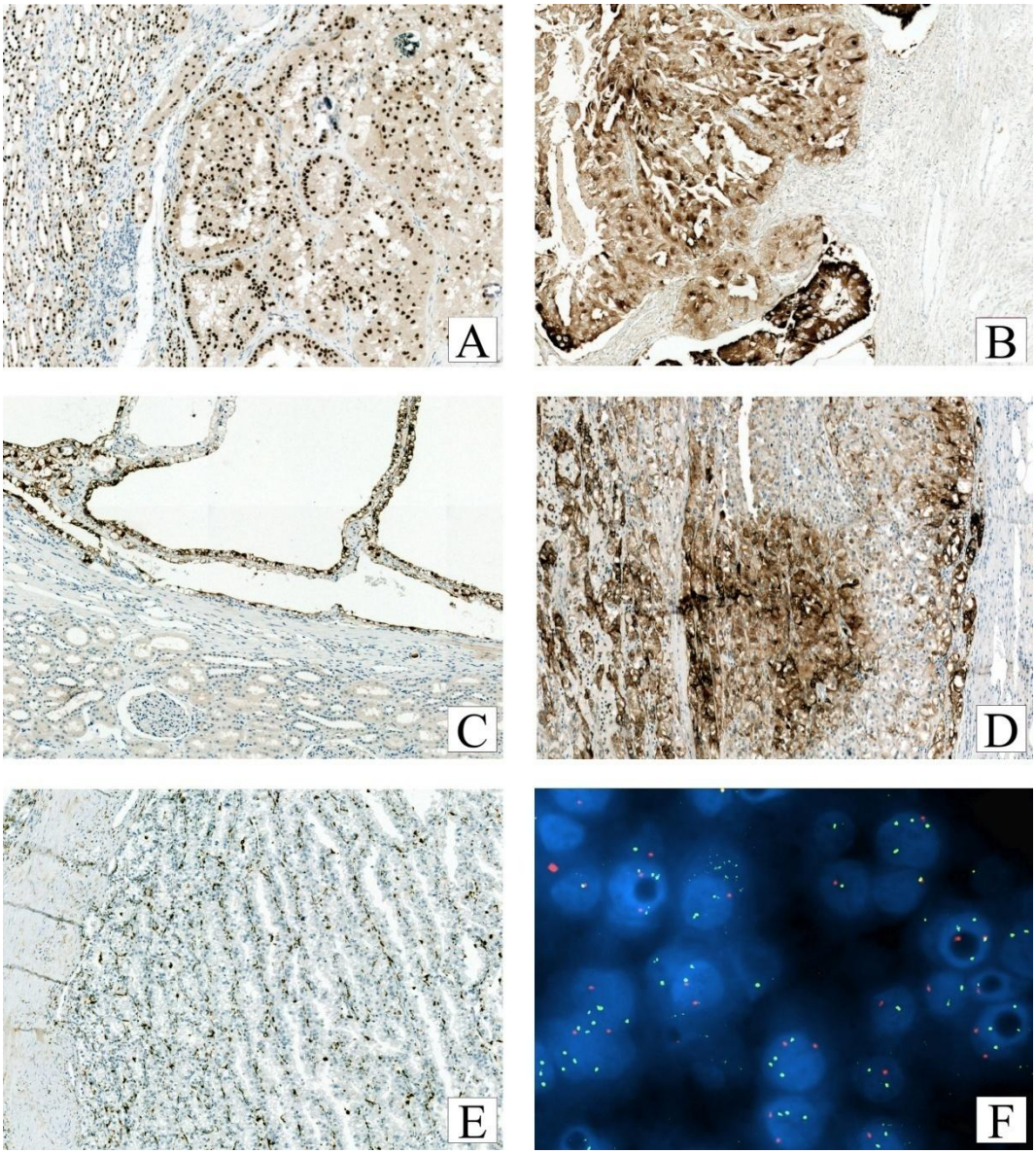

Figure 3. Xp11 renal cell carcinoma showing PAX8 (A), cathepsin K (B), MART1 (C), HMB45 (D) positivity and CD68 (PG-M1) negativity (E). Xp11 carcinoma harbouring both TFE3 translocation and increased gene copy number evaluated by FISH (F).

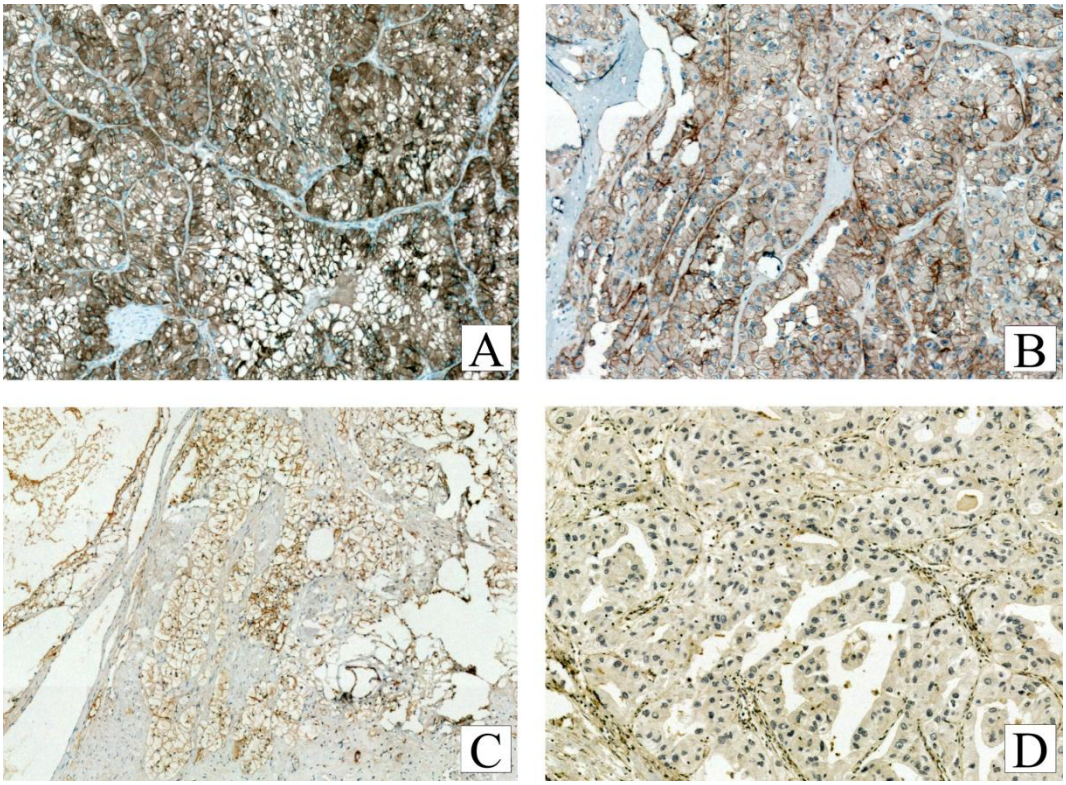

Figure 4. Immunohistochemical expression of MET in Xp11 renal cell carcinoma strong (A), intermediate (B) and mild staining (C). All Xp11 renal cell carcinomas were negative for AXL (D).

FISH results

The results of FISH analysis are detailed in Table 4. All twenty-two Xp11 renal cell carcinomas demonstrated a high frequency of split TFE3 fluorescent signals ranging from 45% to 94% (mean 68%, median 75%). All cases but one were disomic for gene TFE3, TFEB and VEGFA. Case 4 showed an increased number of gene copy of TFE3, TFEB and VEGFA (4-5 signals).

Table 4. FISH results of Xp11 renal cell carcinomas

Case	TFE3 (percentage)	TFE3 status	VEGFA	VEGFA status	TFEB	TFEB status
1	Break (45 %)	Rearranged Disomic	70% 2 signals 30% 4 signals	Disomic	No break	Not rearranged Disomic
2	Break (75 %)	Rearranged Disomic	100% 2 signals	Disomic	No break	Not rearranged Disomic
3	Break (50 %)	Rearranged Disomic	n.a.	n.a.	No break	Not rearranged Disomic
4	Break (85 %) 4-5 signals	Rearranged + GCN gains	90% 4/5 signals	GCN gains	No break 4-5 signals	Not rearranged GCN gains
5	Break (60%)	Rearranged Disomic	90% 2 signals 10% 3 signals	Disomic	No break	Not rearranged Disomic
6	Break (55 %)	Rearranged Disomic	100% 2 signals	Disomic	No break	Not rearranged Disomic
7	Break (60 %)	Rearranged Disomic	100% 2 signals	Disomic	No break	Not rearranged Disomic
8	Break (80 %)	Rearranged Disomic	100% 2 signals	Disomic	No break	Not rearranged Disomic
9	Break (50 %)	Rearranged Disomic	100% 2 signals	Disomic	No break	Not rearranged Disomic
10	Break (55 %)	Rearranged Disomic	85% 2 signals 15% 3 signals	Disomic	No break	Not rearranged Disomic
11	Break (65 %)	Rearranged Disomic	n.a.	n.a.	No break	Not rearranged Disomic
12	Break (75 %)	Rearranged Disomic	100% 2 signals	Disomic	No break	Not rearranged Disomic
13	Break (90 %)	Rearranged Disomic	n.a.	n.a.	No break	Not rearranged Disomic
14	Break (75 %)	Rearranged Disomic	90% 2 signals 10% 3 signals	Disomic	No break	Not rearranged Disomic
15	Break (90 %)	Rearranged Disomic	n.a.	n.a.	No break	Not rearranged Disomic
16	Break (65%)	Rearranged Disomic	100% 2 signals	Disomic	No break	Not rearranged Disomic
17	Break (55%)	Rearranged Disomic	n.a.	n.a.	No break	Not rearranged Disomic
18	Break (75 %)	Rearranged Disomic	n.a.	n.a.	No break	Not rearranged Disomic
19	Break (50 %)	Rearranged Disomic	n.a.	n.a.	No break	Not rearranged Disomic
20	Break (70 %)	Rearranged Disomic	n.a.	n.a.	No break	Not rearranged Disomic
21	Break (80 %)	Rearranged Disomic	90% 2 signals 10% 3 signals	Disomic	No break	Not rearranged Disomic
22	Break (75%)	Rearranged Disomic	n.a.	n.a.	No break	Not rearranged Disomic

n.a.: not available; GCN: gene copy number

t(6;11) renal cell carcinoma and TFEB-amplified renal cell carcinoma

Clinical features

The clinical characteristics of the 10 patients are detailed in Table 5. Five patients were female and five male (F:M ratio, 1:1). The patients' ages at diagnosis ranged from 19 to 80 years (mean 45, median 41). One patient (case 27) had history of non Hodgkin lymphoma treated with chemotherapy and a biopsy was performed when the renal mass was discovered. In case 23, a diagnosis suggesting oncocytoma was made in a core biopsy sample from different institution. Follow up was available for all patients, ranging from 2 to 78 months (mean 39, median 41). Two of them developed metastasis: patient 28 showed paratracheal and pleural metastasis 24 months after the surgery and died of disease after 46 months; patient 29 recurred with nodules in the perinephric fat and pelvic soft tissue after 24 months and he was alive 48 months after the radical nephrectomy. Patient 30, HCV infected, initially presented to the emergency department complaining abdominal pain. He underwent a CT scan, a renal mass was discovered and he underwent radical nephrectomy. Patient 31 and 32 suffered from abdominal pain due to lithiasis of upper urinary tract. In both cases, the renal mass was an incidental finding (Figure 5) and both patients were treated by partial nephrectomy. Follow up was available for all patients, ranging from 14 to 48 months (mean 34, median 33). Patient 30 recurred with multiple nodules adjacent to the pancreatic tail, in the perinephric fat infiltrating the psoas muscle, and in the paravertebral region after 5 months. Sutent (sutinitib) was initiated; however, due to hematological and gastrointestinal toxicities, the treatment was stopped after two weeks. He is currently receiving cabozantinib, and he is alive 14 months after the radical nephrectomy.

Table 5. Clinical and pathological features of renal cell carcinomas with TFEB gene alterations

Case	Age	Gender	Size/Laterality	Stage TNM	Surgery	Follow up
23	19	F	5.5cm/L	pT1bNxMx	Partial nephrectomy	15 months alive
24	54	F	7cm/R	pT1bNxMx	Radical nephrectomy	36 months alive
25	20	F	9,5cm/R	pT2aNxMx	Radical nephrectomy	36 months alive
26	55	M	3cm/R	pT1aNxMx	Partial nephrectomy	78 months alive
27	34	M	7cm/L	pT1bNxMx	Partial nephrectomy	30 months alive
28	42	F	10cm/L	pT3aN0M1	Radical nephrectomy	metastasis after 24 months, dead after 46 months
29	33	M	8cm/L	pT3aNxM1	Radical nephrectomy	perinephric nodules after 24 months, 48 months alive
30	69	M	7cm/L	pT2aNxMx	Radical nephrectomy	perinephric nodules after 5 months, 14 months alive
31	41	F	3cm/L	pT1aNxMx	Partial nephrectomy	20 months alive
32	79	M	10cm/L	pT2aNxMx	Partial nephrectomy	18 months alive

F: female, M: male, R: right, L: left

Pathological features

The tumors ranged in size from 3 to 10 cm (mean and median 7) (Figure 5). All but one was solid and tan mass (Figure 5), the smallest tumor was solid and cystic (Figure 5). Grossly, in the cases treated by radical nephrectomy, renal vein invasion was not identified. The histological features are described separately for completeness.

Case 23

A discontinuous thick pseudocapsule with dystrophic calcification was present. The tumor was composed of epithelioid cells with eosinophilic and focally clear cytoplasm and small nucleoli (G2 by ISUP/WHO 2016) mainly arranged in solid-alveolar architecture (Figure 6). Areas with tubular and microcystic pattern were seen. Neither necrosis nor mitotic activity was found (<1 per 10HPF).

Case 24

A discontinuous pseudocapsule was present. The neoplasm was mainly composed of nests and tubules of polygonal cells with well-defined cell borders, clear cytoplasm and central round nuclei with prominent nucleoli (G3 by ISUP/WHO 2016). Additional areas showing cells with granular and eosinophilic cytoplasm were present. Tubular and micropapillary structures were also

observed. Smaller cells with dark nuclei clustering around hyaline material were focally seen. Mitotic figures were occasionally encountered (0-1 per 10 HPF). No necrosis was found.

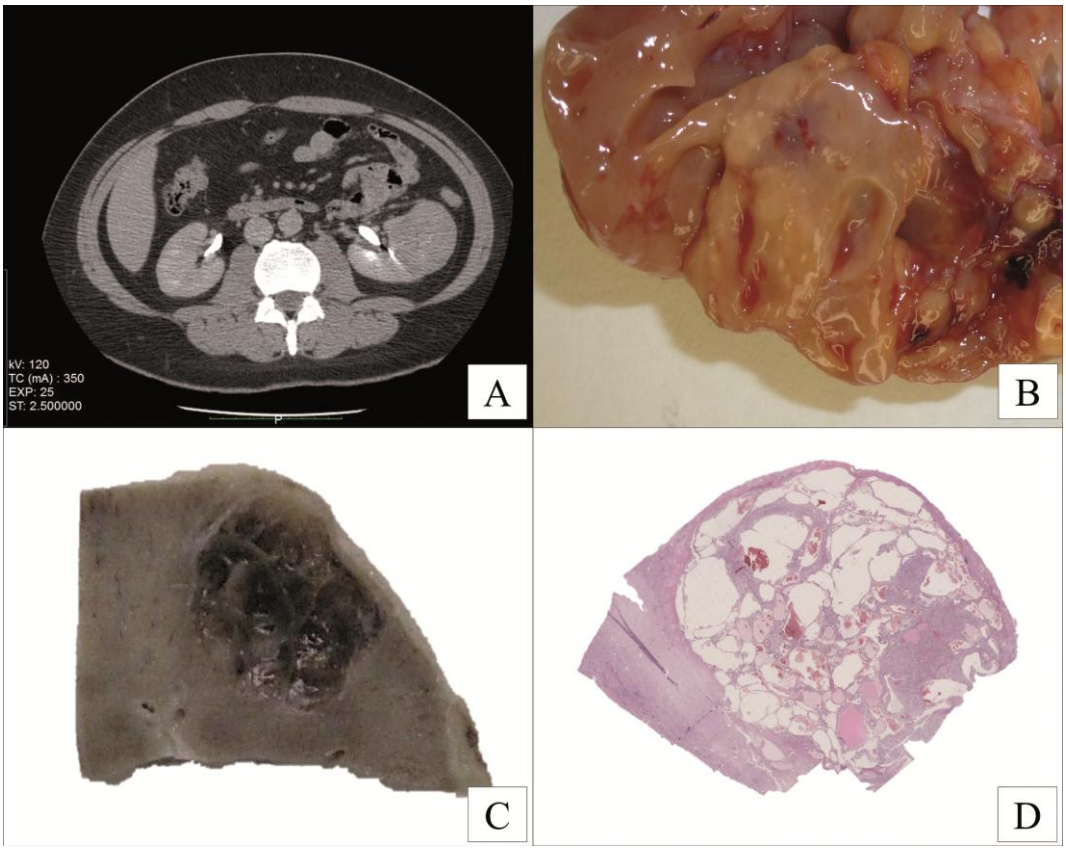

Figure 5. The most common macroscopic appearance of t(6;11) renal cell carcinoma: a solid (A) and tan mass (B). Only one tumor displayed a solid and cystic architecture (C-D).

Case 25

The tumor was partially circumscribed by a fibrous pseudocapsule and made up of granular eosinophilic polygonal cells with conspicuous nucleoli (G2 by ISUP/WHO 2016) arranged in solid and solid/alveolar architecture. At low power magnification, smaller lymphocyte-like cells grouped around collagenous spherules formed by basement membrane material were easily observed. Additional areas with microcysts were focally present. A few psammoma bodies and 1 mitotic figure per 10 HPF were found. No necrosis was observed.

Case 26

The tumor was solid and cystic and well-delineated by a pseudocapsule. The cells lining the cysts showed abundant vacuolated clear and eosinophilic cytoplasm with round nuclei and pinpoint nucleoli (G2 by ISUP/WHO 2016). Brownish pigment and psammoma bodies were extensively present. Mitotic figures were occasionally seen (0-1 per 10 HPF). Necrosis was absent.

Case 27

The biopsy showed an epithelial neoplasm made up of sheets of small cells with round hyperchromatic nuclei and eosinophilic cytoplasm. In the resected specimen, the tumor consisted of a mixture of epithelioid cells with clear and granular eosinophilic cytoplasm and indistinct nucleoli (G2 by ISUP/WHO 2016) (Figure 6). Architecturally, solid areas, microcystic and papillary changes (Figure 6) and bony metaplasia were observed. Areas of hyalinized stroma with calcification and hyalinized vessels were present (Figure 6). Mitotic figures were occasionally seen (1 per 10 HPF). No necrosis was observed.

Case 28

Primary tumor: The tumor showed pushing margins and it was partially delineated from renal parenchyma by a pseudocapsule. However, an infiltrative growth pattern in the perinephric fat was focally present. The neoplastic cells were large and epithelioid with abundant clear cytoplasm and enlarged hyperchromatic nucleoli (G3 by ISUP/WHO 2016) (Figure 7). Hyaline sclerosis with eosinophilic material around vessels, dystrophic calcification and bony metaplasia were present throughout the tumor. Minimal mitotic activity was encountered (<1 per 10HPF) in most of the neoplasm. Focal necrosis was seen (Figure 7). An additional area of neoplastic overgrowth was found. This area measured roughly 1.5 cm and was characterized by small eosinophilic cells (G3 by ISUP/WHO 2016) with necrosis and higher mitotic activity (15 per 10 HPF). Eight hilar lymph nodes were examined and were negative for tumor metastasis.

Metastatic tumor: Biopsy material of pleural metastasis was available for histological characterization and consisted of clear cells with distinct borders and small round nuclei (Figure 7). No necrosis or mitotic activity was observed.

Case 29

Primary tumor: The tumor was characterized by cells with clear to eosinophilic cytoplasm and small nuclei (G2 by ISUP/WHO 2016) arranged in solid-alveolar pattern and focal papillary architecture. A few mitotic figures were encountered (3 per 10 HPF). Necrosis was absent.

Metastatic tumor: The same features were observed in metastatic nodules in perinephric fat and pelvis (Figure 7). Higher mitotic activity was found (5 per 10 HPF).

Case 30

A discontinuous thick fibrous pseudocapsule was present. The tumor was predominantly composed of epithelioid cells with eosinophilic and focally clear cytoplasm and prominent nucleoli (G3 by ISUP/WHO 2016) mainly arranged in solid-alveolar architecture (Figure 8). In some areas smaller epithelioid clear cells were observed. Hemosiderin-laden histiocytes and extensive tumoral necrosis were noted.

Case 31

The tumor was well-delineated by a fibrous pseudocapsule and characterized by a tubulocystic pattern with a thin eosinophilic fluid material filling the cystic spaces. The single layer of cuboidal cells lining the tubules and the cysts showed abundant granular eosinophilic cytoplasm with round nuclei and pinpoint nucleoli (G2 by ISUP/WHO 2016) (Figure 8). Few macrophages bearing hemosiderin pigment were observed. Neither necrosis nor mitotic activity was found (<1 per 10HPF).

Case 32

A thick fibrous pseudocapsule was present. The solid area of the neoplasm was mainly composed of medium-sized polygonal cells with eosinophilic and more rarely clear cytoplasm arranged in a alveolar and less frequently tubular-acinar or pseudopapillary (Figure 8). The nuclei showed prominent nucleoli (G3 by ISUP/WHO 2016). Mitotic figures were occasionally encountered (0-1 per 10 HPF). Tumoral necrosis and hemorrhage were found.

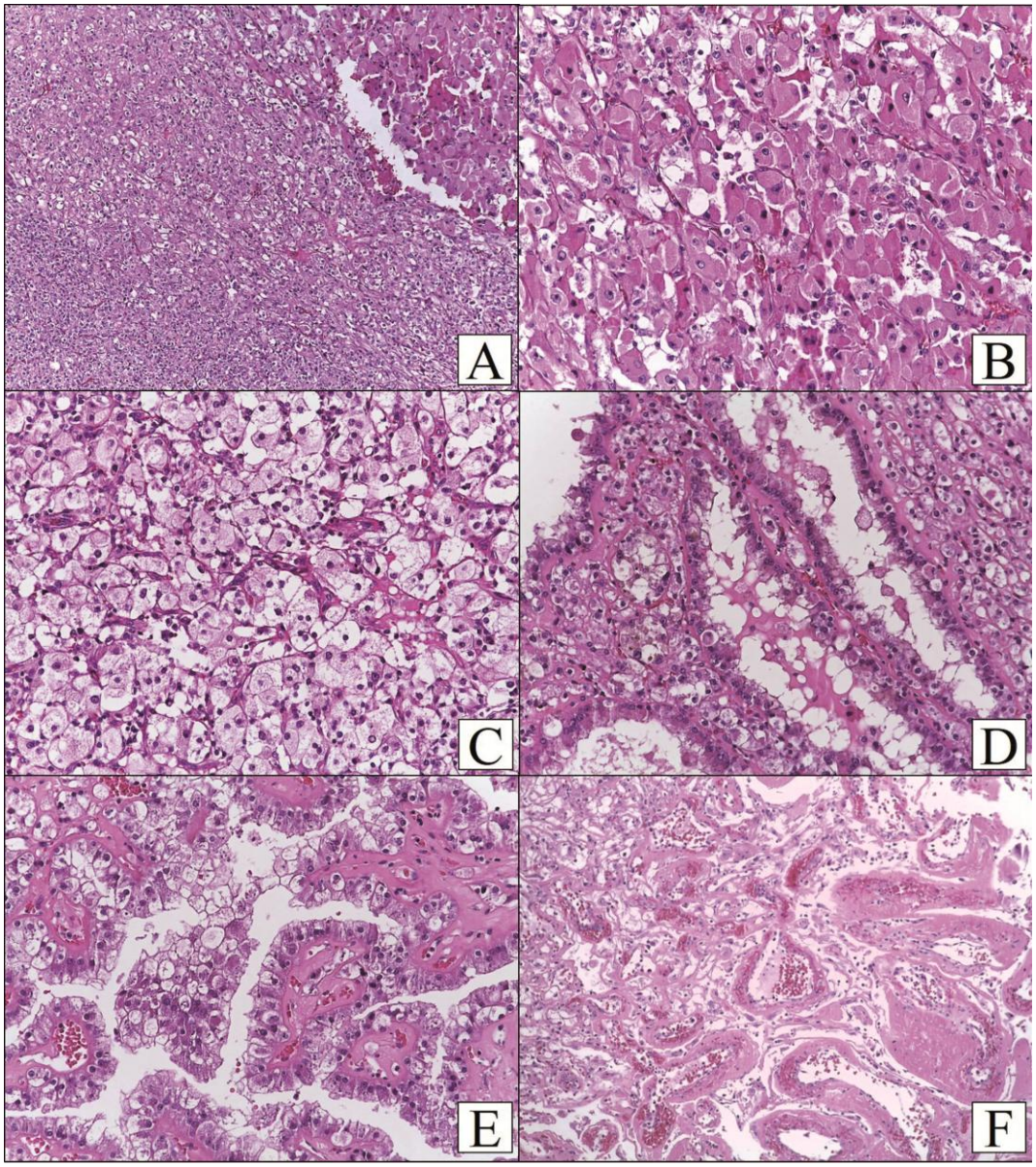

Figure 6. Different histologic appearances of t(6;11) renal cell carcinoma. Large epithelioid eosinophilic (A, B) and clear cells. Areas with microcystic (D) and papillary (E) pattern. Hyaline sclerosis with eosinophilic material around vessels, a pattern reminiscent of epithelioid angiomyolipoma (F).

Figure 7. t(6;11) renal cell carcinomas with aggressive behavior. The broad and epithelioid clear cells of case 6 (A) with focal necrosis (B). A biopsy of pleura showing clear cell with distinct borders and small round nuclei (C). Nodules in perinephric fat displayed a solid-alveolar pattern, note the clear to eosinophilic epithelioid cells (insert) (D). Expression of Melan-A (E) and cathepsin K (F) in tumor metastasis.

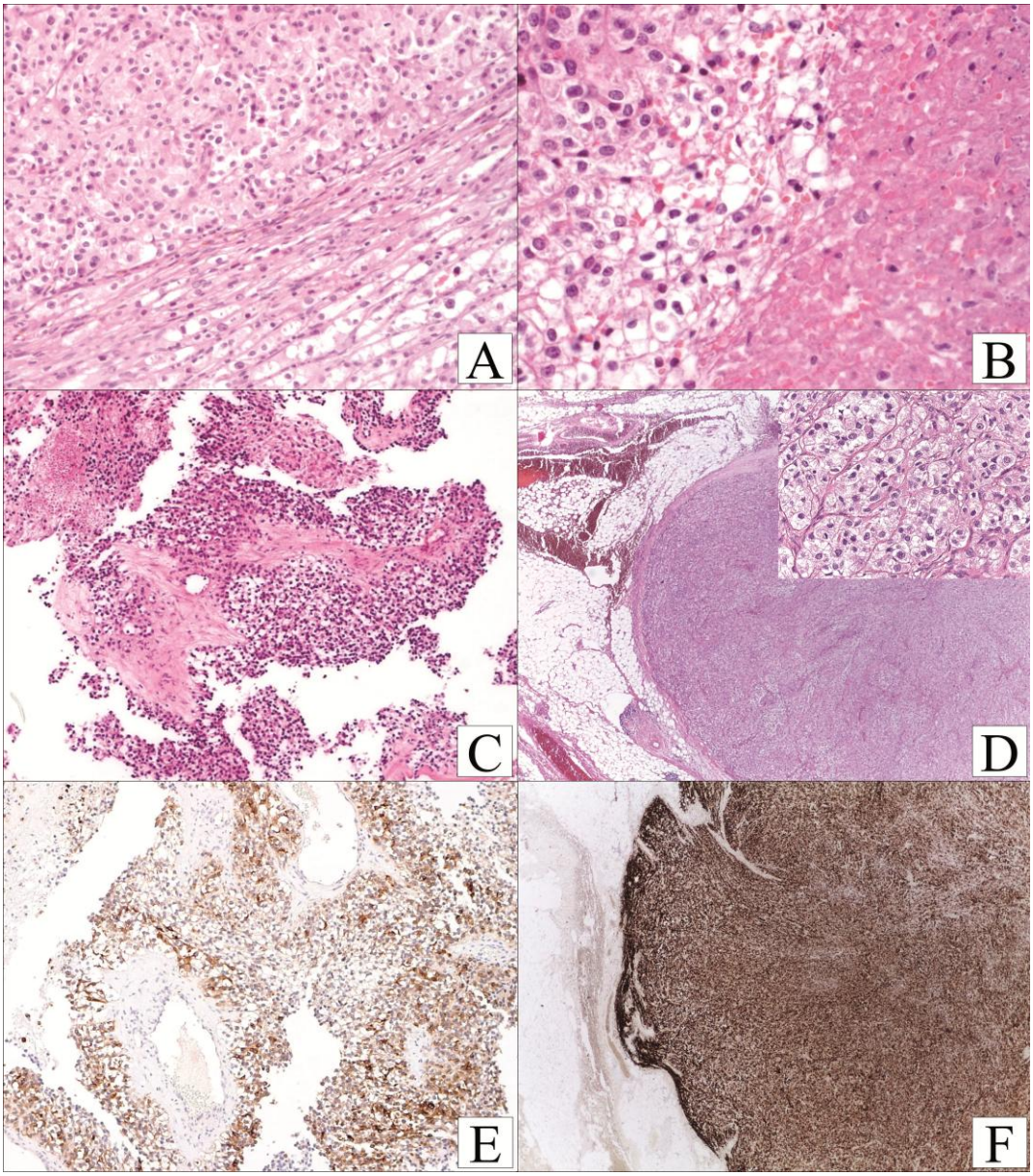

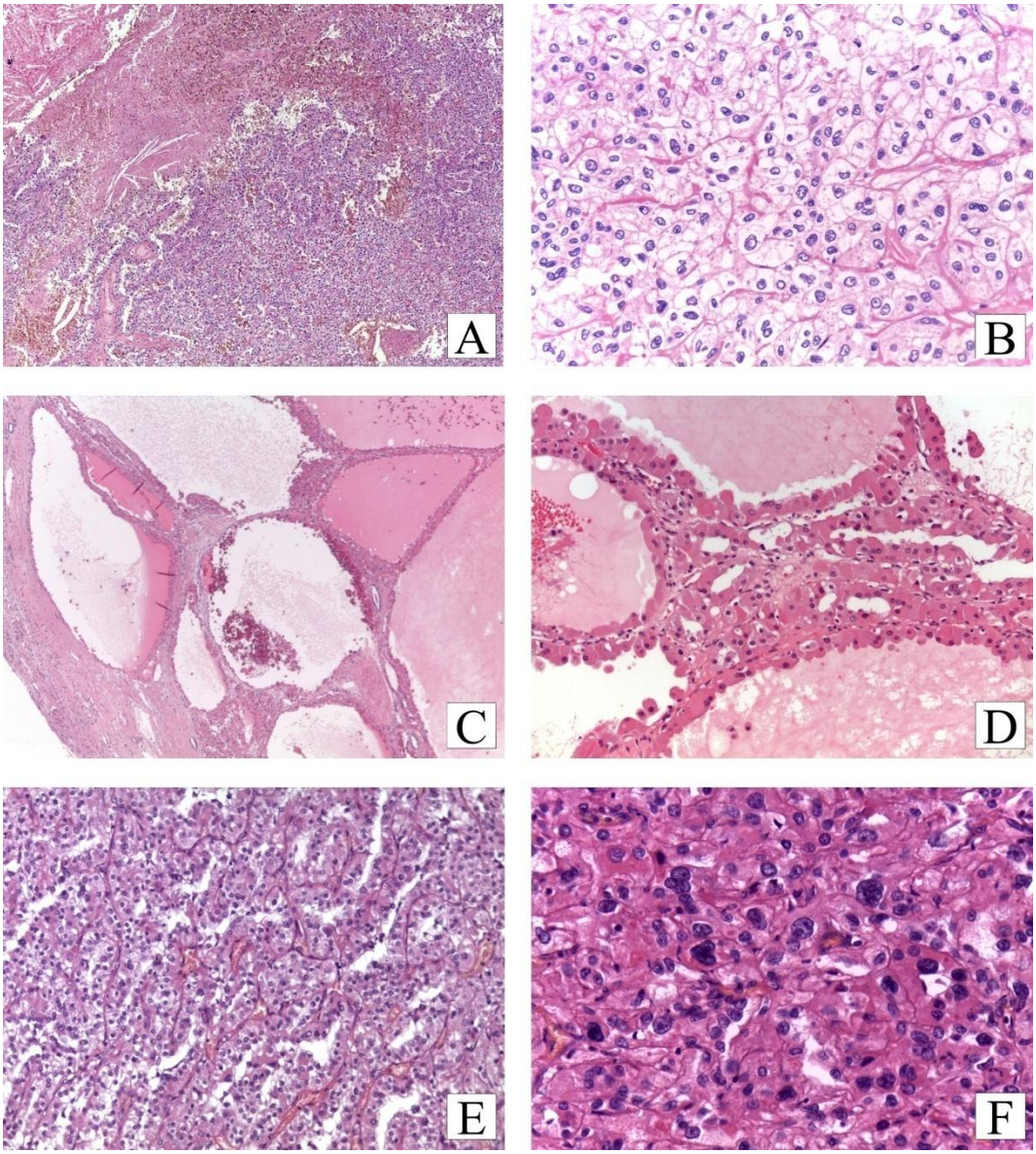

Figure 8. Histologic features of TFEB-amplified renal cell carcinomas. Low power view of case 8 shows a neoplasm with tumoral necrosis composed of epithelioid cells with eosinophilic (A) and clear cytoplasm and prominent nucleoli (B). The tumor of case 9 was composed of variably-sized cysts (C) lined by a single layer of cuboidal cells with eosinophilic cytoplasm and small round nuclei (D). Two different architectures of case 10 were present, tubular-acinar (E) and solid areas made up of medium-sized polygonal cells with eosinophilic cytoplasm and prominent nucleoli (F).

Immunohistochemical features

The immunohistochemical results are tabulated in Table 6. All t(6;11) renal cell carcinomas were positive for cathepsin K, and CD68 (KP1 clone) whereas expression for Melan-A and CK8-18 was observed in all tumors with different percentages (Figure 7). Staining for PAX8 and HMB45 was found in 7 of 8 tumors and in 6 of 8 tumors respectively. In the overgrowth area of case 23, the immunohistochemical expression of the markers was the same. Both TFEB-amplified renal cell carcinomas immunostained for PAX8, CK8-18 and cathepsin K, whereas just one tumor was positive for HMB45 and Melan-A. CD68 (PG-M1) was negative in all tumors (Figure 10). Staining for MET was observed in 5 of 7 t(6;11) renal cell carcinomas tested whereas none of the 7 tumors expressed AXL.

All seven pure epithelioid PEComa /epithelioid angiomyolipomas labeled for cathepsin K, melanocytic markers (HMB45 and Melan-A) and CD68 (both PG-M1 and KP1 clones) and were negative for PAX8 (Figure 9).

Table 6. Immunohistochemical results of renal cell carcinomas with TFEB gene alterations

Case	PAX8	CK8-18	Cathepsin k	HMB45	Melan A	CD68(PG-M1)	MET	AXL
23	80% +	15%	100% +	5% +	80%+	neg	50% ++/ 20% +	neg
24	80% +	30%	70% +	5% +	80% +	neg	neg	neg
25	10% +	70%	70% +	5% +	20% +	neg	5% +	neg
26	70% +	30%	100% +	5% +	80% +	neg	40% ++/ 20% +	neg
27	60% +	10%	90% +	5% +	80% +	neg	70% ++/ 20% +	neg
28	20% +	5%	80% +	10% +	80% +	neg	5% +	neg
29	neg	10%	100% +	neg	5% +	neg	20% +	neg
30	30%+	40%	40%+	neg	90%+	neg	n.a.	n.a.
31	50%+	50%	100% +	1%+	5%+	neg	n.a.	n.a.
32	50%+	20%	10%+	neg	neg	neg	n.a.	n.a.

n.a.: not available

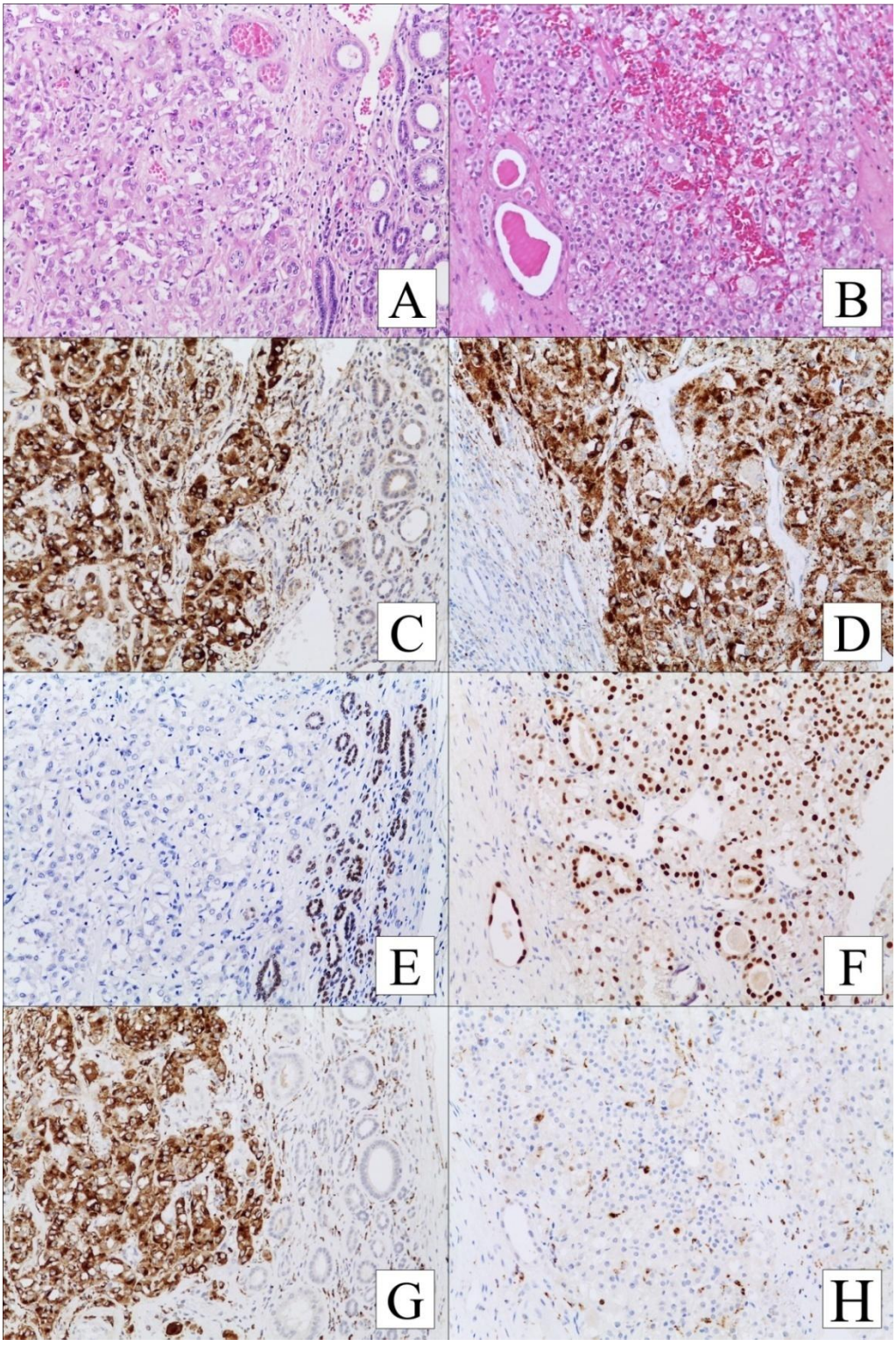

Figure 9. t(6;11) renal cell carcinoma (A) showing cathepsin K (C) and PAX8 (E) positivity and CD68 PG-M1 negativity (G). Pure epithelioid PEComa/epithelioid angiomyolipoma (B) expressing cathepsin K (D). On the contrary of t(6;11) renal cell carcinoma, pure epithelioid PEComa/epithelioid angiomyolipoma was negative for PAX8 (F) but positive for CD68 PG-M1(H).

FISH results

All eight t(6;11) renal cell carcinomas and two metastasis demonstrated a high frequency of split TFEB fluorescent signals (Figure 11) ranging from 61% to 94% (mean 74%, median 75%) detailed in Table 7. In all these samples the distance of red and green signals was greater than twice signal diameter. In two tumors (case 28 and 29) increased gene copy number was observed (3-5 fluorescent signals per neoplastic nuclei) (Figure 11). In case 28, the increased number of fluorescent signals was mainly observed in the overgrowth nodule. Both tumors showed increased number of CEP6 (3-4 copies) whereas the remaining four tumors were disomic. The remaining three cases showed a high level of *TFEB* gene amplification (>10 copies of fluorescent signals), one with *TFEB* rearrangement, the other two without evidence of rearrangement (Figure 10). *VEGFA* was amplified in all three cases with *TFEB* amplification. In two of them (case 30 and case 32), the levels of amplification of VEGFA and TFEB were identical, whereas in case 31 the level of amplification of *VEGFA* was lower than the level of *TFEB* (Table 7).

None of the 37 control tumors showed split TFEB fluorescent signals. Minimally split fluorescent signals in which fluorescent signals were separated by a signal diameter were occasionally observed (mean 3.8%, median 3%, range from 0% to 10%); these were considered artifactual and no significant.

Table 7. Molecular results of renal cell carcinomas with TFEB gene alterations

Case	TFEB FISH	TFE3 FISH	CEP6	VEGFA FISH	VEGFA RNAscope	TFEB status by FISH	VEGFA status by FISH	VEGFA status by RNAscope
23	Break (74%)	no break	2-3 signals	2-3 signals	4	rearranged	disomic	positive
24	Break (80%)	no break	2 signals	2 signals	1	rearranged	disomic	negative
25	Break (75%)	no break	2 signals	2-3 signals	1-2	rearranged	disomic	negative
26	Break (65%)	no break	2 signals	2 signals	3-4	rearranged	disomic	positive
27	Break (78%)	no break	2-3 signals	2-3 signals	4	rearranged	disomic	positive
28	Break (94%) 3-5 signals	no break 3 signals	3-4 signals	3 signals	4	rearranged + GCN gains	GCN gains	positive
29	Break (61%) 3-5 signals	no break	3-4 signals	4-5 signals	3-4	rearranged + GCN gains	GCN gains	positive
30	Break (75%) >10 signals	no break	2 signals	> 10 signals	3	rearranged + amplified	amplified	positive
31	No break >10 signals	no break	3 signals	> 10 signals (10% of nuclei) 6 signals (90% of nuclei)	4	amplified	amplified	positive
32	No break >10 signals	no break	4 signals	> 10 signals (80% of nuclei) 6 signals (20% of nuclei)	3-4	amplified	amplified	positive

GCN: gene copy number

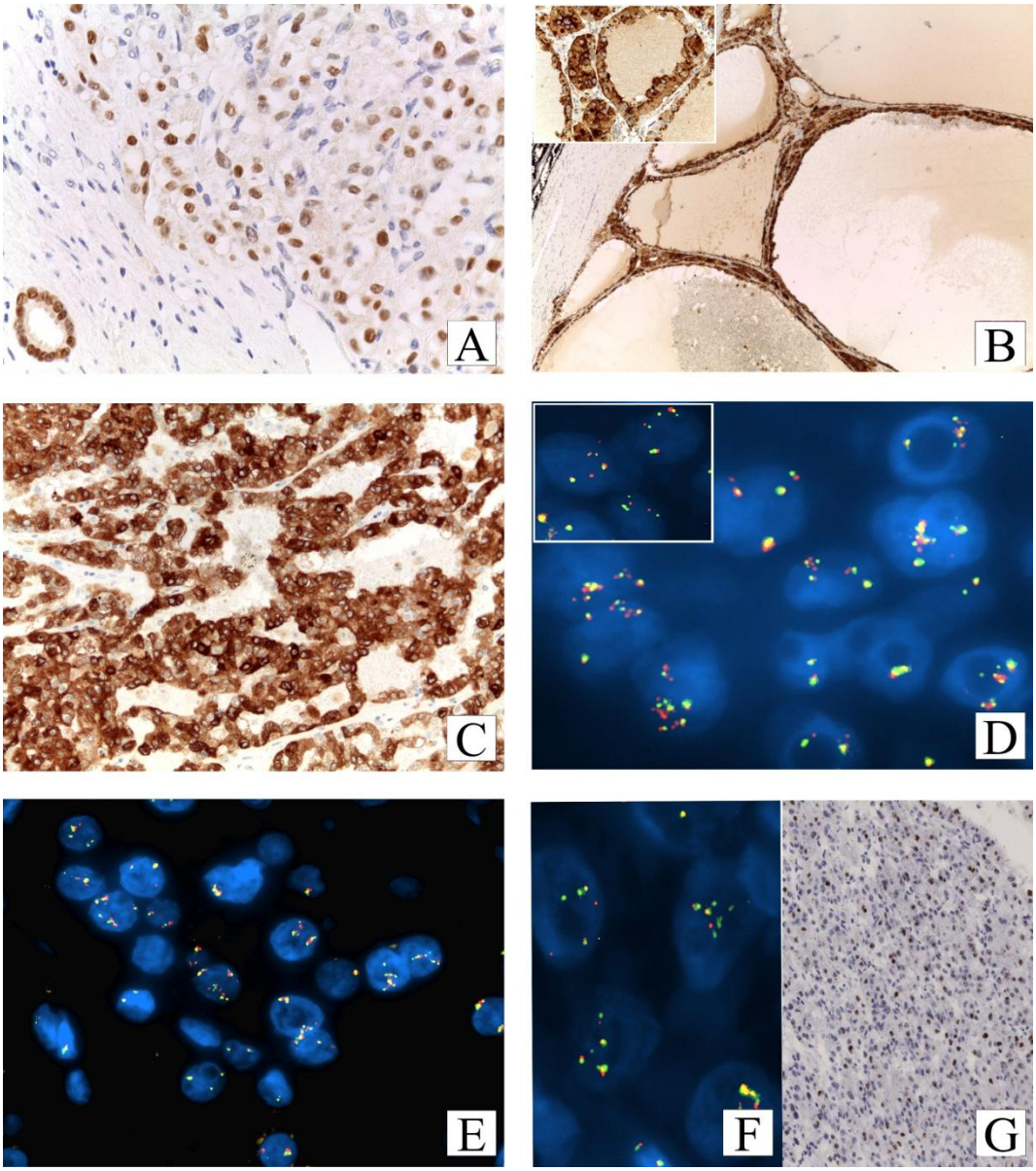

Figure 10. Immunophenotype of TFEB-amplified renal cell carcinomas. PAX 8 was positive in the neoplastic cells of case 30 (A). The cells lined the cysts of case 31 were strongly positive for cathepsin K (high magnification in the insert) (B). Staining for Melan-A was diffusely present in the tumor cells of case 32 (C). Fluorescence *in situ* hybridization result of case 30 shows TFEB amplification (D). The green and red signals are split apart demonstrate the break of the *TFEB* gene (insert). *TFEB* gene amplification of case 32 (E) with identical level of amplification of *VEGFA* (F) and high VEGFA mRNA expression (G).

RNAscope results

Overall, VEGFA mRNA expression was observed in 8 of 10 (80%) renal cell carcinomas with *TFEB* gene alteration (Table 7). Of these 8 cases positive for VEGFA staining, three cases showed high level *TFEB* amplification, one case showed *TFEB* rearrangement with increased *TFEB* gene copy number, while four showed *TFEB* gene rearrangement without increased copy number (Figure 10). None of the papillary renal cell carcinomas, chromophobe renal cell carcinomas and oncocytomas demonstrated a positive staining for VEGFA whereas two of three clear cell renal cell carcinomas showed a high VEGFA mRNA expression.

Cytogenetic results

Fresh tumor samples were available for karyotype analysis in 2 of 10 tumors (case 24 and case 27). The karyotype result of case 24 was previously reported[28]. In case 27, all the analyzed cells showed the translocation t(6;11)(p21;q12) (Figure 11). A subset of these cells, about 20%, showed additional rearrangements including monosomy of chromosome 22 and translocation of almost its entire long arm on the short arm of chromosome 8, as showed by FISH results in which both the probes mapping in 22q11.2 and q13.3 are located on the rearranged chromosome 8.

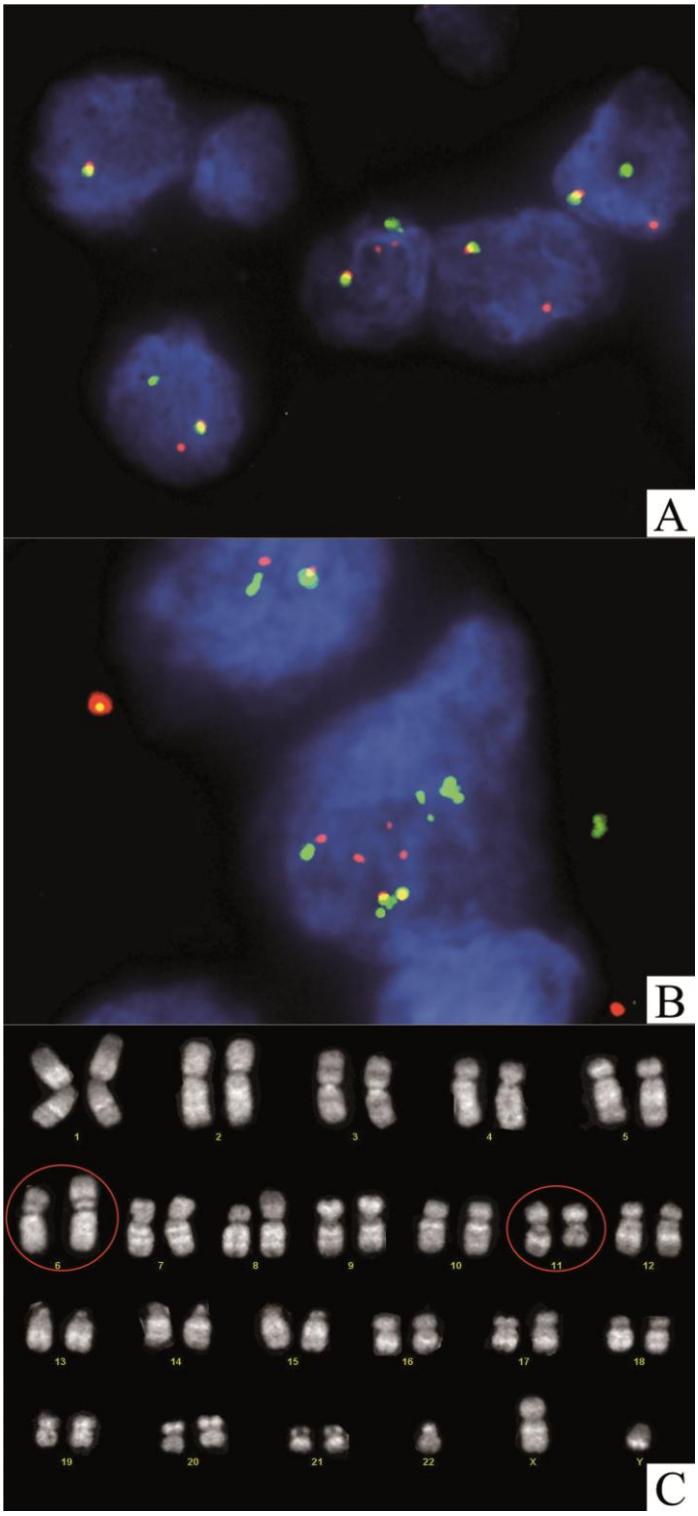

Figure 11. All t(6;11) renal cell carcinomas demonstrated *TFEB* rearrangement (A). Note the increased number of fluorescent signals in cases with aggressive behavior (B). Representative QFQ banded karyotype of the tumor (case 27): 46, XY, t(6;11)(p21;q12) karyotype (C).

Literature review and comparison of aggressive and non-aggressive t(6;11) renal cell carcinoma

Aggressive t(6;11) renal cell carcinoma. The results of the literature review [14, 20, 21, 26, 29-32] and the new two aggressive cases of t(6;11) renal cell carcinoma are summarized in Table 8. The mean age of these patients was 46 years and the median 42 years (range from 33 to 77). There was a male predominance (8M, 3F), with a male-to-female ratio of roughly 2.6:1. The tumors' size ranged from 3 to 27 cm (mean 12, median 10). Follow up for these cases ranged from 3 to 120 months (mean 59, median 48). Among the eleven patients, four died for disease. All of them developed metastasis. In decreasing order of frequency, the metastatic sites were lung (3 cases), bone (3 cases), liver (2 cases), lymph nodes (2 cases), perinephric fat and pelvic soft tissue (1 case), vagina (1 case). In one patient, the site of metastasis was not specified.

Non-aggressive t(6;11) renal cell carcinoma. The new cases of t(6;11) renal cell carcinoma and the results of the literature review[14, 19-23, 26, 28, 30, 31, 33-45] are presented in Table 9. Overall, 53 cases of t(6;11) renal cell carcinoma were found. The mean age of these patients was 30 years and the median 29 years (range from 3 to 68). There was no gender predominance (26M, 25F). The tumors' size ranged from 1 to 19 cm (mean and median 7). When follow up was available, it ranged from 2 to 60 months (mean 27 and median 25).

Comparison of aggressive and non-aggressive t(6;11) renal cell carcinoma. There is a statistically significant difference in age and tumors' size between aggressive and non-aggressive tumors. The aggressive tumors occur in older patients ($p=0.007$) and tend to be larger ($p=0.04$). Although there is a prevalence of aggressive t(6;11) renal cell carcinoma in men, no significant difference in gender was found ($p=0.32$).

Table 8. Aggressive t(6;11) renal cell carcinomas

Case	References	Age	Gender	Size (cm)	Stage TNM	Karyotype/FISH	Follow up	Notes
1	Camparo et al., 2008	36	M	20	pT3bN2M1	NA*	dead after 3 months	multiple metastasis
2	Ishihara et al., 2011	45	M	7	pT3aN1M1	NA	7 months alive	lung and vertebral metastasis
3	Argani et al., 2012	42	M	27	pT3NxM1	break apart probe	NA	liver metastasis
4	Argani et al., 2012	60	M	14	pT3bN0M1	break apart probe	NA	liver metastasis + IVC thrombus
5	Inamura et al., 2012	37	M	NA	NA	t(6;11)(p21.1;q12 13)	dead after 120 months	lung metastasis
6	Peckova et al., 2014	77	F	12	pT3NxM1	RT-PCR + break apart	dead after 2,5 months	adrenal gland and lung metastasis
7	Smith et al., 2014	34	M	3	pT1NxM1	break apart probe	96 months alive	rib metastasis
8	Lilleby et al., 2015	42	M	NA	NA	break apart probe	97 months alive	vertebral and rib metastasis
9	Argani et al., 2016	61	F	19	pT4N0M1	break apart probe	18 months alive	vaginal metastasis
10	Present series (case 28)	42	F	10	pT3aN0M1	break apart probe	dead after 46 months	lung metastasis
11	Present series (case 29)	33	M	8	pT3aNxM1	break apart probe	48 months alive	perinephric and pelvic soft tissue tissue nodules

M: male, F: female, NA: not available, IVC: inferior vena cava

Table 9. Non aggressive t(6;11) renal cell carcinomas

Case	References	Age	Gender	Size (cm)	Stage TNM	Karyotype/ FISH	Follow up	Notes
1	Argani et al., 2001 Davis et al., 2003 Argani et al., 2005	18	M	7	pT1bNxMx	t(6;11)(p21.1;q12)	18 months	
2	Argani et al., 2001 Argani et al., 2005 Martignoni et al., 2009	10	M	12	pT2NxMx	t(6;11)(p21.1;q12)	26 months	
3	Kuiper et al., 2003 Dijkhuizen et al., 1996	42	F	NA	NA	t(6;11)(p21;q13)	NA	
4	Kuiper et al., 2003 Dijkhuizen et al., 1996	17	F	NA	NA	t(6;11)(p21;q13)	NA	
5	Kuiper et al., 2003 Argani et al., 2005 Martignoni et al., 2009	14	F	4.5	pT1bNxMx	t(6;11)(p21;q13)	NA	
6	Davis et al., 2003 Argani et al., 2005	18	F	2.8	pT1aNxMx	t(6;11)(p21.1;q12)+ break apart	18 months	
7	Argani et al., 2005 Martignoni et al., 2009	20	F	9.5	pT2NxMx	RT-PCR	30 months	
8	Argani et al., 2005 Geller et al., 2008 Martignoni et al., 2009	9	F	2	pT1aNxMx	RT-PCR	NA	post chemotherapy (nephroblastoma)
9	Argani et al., 2005 Martignoni et al., 2009	33	M	6	pT1bNxMx	RT-PCR	NA	
10	Argani et al., 2006 Martignoni et al., 2009	6	F	5	pT1bNxMx	t(6;11)(p21;q12)	3 months	post chemotherapy (nephroblastoma)
11	Pecciarini et al., 2007 Martignoni et al., 2009 Petterson et al., 2014 Present series (case 2)	54	F	7	pT1bNxMx	t(6;11)(p21;q12)	36 months	
12	Camparo et al., 2008	34	F	15	pT2N0M0	t(6;11)(p21;q13)	50 months	
13	Hora et al., 2009 Petterson et al., 2012 Peckova et al., 2014	22	M	4	pT1bNxMx	NA	40 months	
14	Hora et al., 2009 Petterson et al., 2012 Peckova et al., 2014	24	F	13.6	pT2NxMx	NA*	18 months	pregnant
15	Hora et al., 2009	39	F	1	pT1aNxMx	NA	13 months	
16	Zhan et al., 2010	26	M	4.3	pT1bNxMx	RT-PCR	6 months	
17	Malouf et al., 2011	NA	NA	NA	NA	NA*	NA	
18	Suarez Villa et al., 2011	22	M	10	pT2NxM0	NA*	NA	
19	Argani et al., 2012	14	F	NA	NA	break apart probe	NA	
20	Argani et al., 2012	37	M	4	pT1aNxMx	break apart probe	NA	

21	Argani et al., 2012	3	F	2	pT1aNxMx	break apart probe	NA	
22	Argani et al., 2012	58	F	3	pT1aNxMx	break apart probe	NA	
23	Argani et al., 2012	34	M	1.8	pT1aNxMx	break apart probe	NA	end stage kidney
24	Argani et al., 2012	25	M	15	pT2NxMx	break apart probe	NA	
25	Inamura et al., 2012	57	M	10.2	pT2NxMx	NA*	8 months	
26	Inamura et al., 2012	47	M	3.2	pT1aNxMx	t(6;11)(p21.1;q12 13)	12 months	
27	Petterson et al., 2012 Peckova et al., 2014 Present series (case 3)	20	F	9.5	pT2NxMx	t(6;11) (p21;q12)	60 months	
28	Petterson et al., 2012 Peckova et al., 2014	54	F	7	pT1bNxMx	t(6;11) (p21;q12)	36 months	
29	Rao et al., 2012	31	F	9	pT2NxMx	break apart probe	6 months	
30	Rao et al., 2012	21	M	4	pT1aNxMx	break apart probe	22 months	
31	Rao et al., 2012	37	F	3	pT1aNxMx	break apart probe	34 months	
32	Rao et al., 2012	36	F	2.5	pT1aNxMx	break apart probe	NA	
33	Rao et al., 2012	30	M	9	pT2NxMx	break apart probe	31 months	
34	Rao et al., 2012	29	F	4.5	pT1bNxMx	break apart probe	55 months	
35	Rao et al., 2012	30	M	4	pT1aNxMx	break apart probe	36 months	
36	Zhong et al., 2012	17	M	19	pT2NxMx	NA*	NA	
37	Rao et al., 2013	68	M	2,5	pT1aNxMx	break apart probe	23 months	
38	Peckova et al., 2014	15	M	10	pT2NxMx	break apart probe	12 months	
39	Matsuura et al., 2014	40	M	NA	NA	MALAT1(alpha)–TFEB	NA	
40	Smith et al., 2014	NA	NA	NA	NA	break apart probe	NA	
41	Smith et al., 2014	44	M	7.8	pT2NxMx	break apart probe	NA	
42	Smith et al., 2014	9	M	4	pT1aNxMx	break apart probe	NA	
43	Smith et al., 2014	3	F	NA	NA	break apart probe	NA	
44	Smith et al., 2014	23	M	10	pT2NxMx	break apart probe	NA	
45	Smith et al., 2014	9	F	9	pT2NxMx	break apart probe	NA	
46	Smith et al., 2014	46	M	15	pT2NxMx	break apart probe	NA	
47	Smith et al., 2014	68	M	2.8	pT1aNxMx	break apart probe	NA	
48	Smith et al., 2014	62	M	3	pT1aNxMx	break apart probe	NA	
49	Arneja et al., 2015	11	M	13.7	pT2NxMx	break apart probe	NA	
50	Argani et al., 2016	61	M	2.7	pT1aNxMx	break apart probe	NA	
51	Present series (case 26)	55	M	3	pT1aNxMx	break apart probe	78 months	
52	Present series (case 27)	34	M	7	pT1bNxMx	break apart probe	30 months	
53	Present series (case 23)	19	F	5.5	pT1bNxMx	break apart probe	2 months	
M: male, F: female, NA: not available								

DISCUSSION

In this study, we collected a large series of MiT family translocation renal cell carcinoma and we analyzed 1) immunohistochemical diagnostic markers since the differential diagnosis is challenging, especially with pure epithelioid PEComa/epithelioid angiomyolipoma; 2) a proper cut-off by fluorescence in situ hybridization to reach the correct diagnosis; 3) possible predictive markers in tumor tissue for target therapy.

We have evaluated the possible usefulness of CD68 as immunohistochemical marker to differentiate MiT family translocation renal cell carcinoma from pure epithelioid PEComa /epithelioid angiomyolipoma. Distinguishing those two entities is clinically important since mTOR inhibitors are a therapeutic option for the latter [46], and, in our experience, the differential diagnosis of MiT family translocation renal cell carcinoma, especially t(6;11) renal cell carcinoma with pure epithelioid PEComa /epithelioid angiomyolipoma is the most difficult. Both tumors are composed of medium and large cells with clear or faintly granular eosinophilic cytoplasm and enlarged nuclei usually with prominent nucleoli. As described in this study and previously reported [42, 47], t(6;11) renal cell carcinoma may show hyalinized areas with thick-walled vessels mimicking the abnormal blood vessels in the angiomyolipoma. Moreover, the two entities share the immunohistochemical expression of melanocytic markers and cathepsin K and both are often negative for cytokeratin [48]. Staining for PAX8 has been demonstrated a useful tool in this challenging diagnosis. In this study we found that all but three FISH-confirmed MiT family translocation renal cell carcinomas were positive for PAX8 and 7 pure epithelioid PEComa/epithelioid angiomyolipomas were consistently negative. As we previously reported [24], either CD68 (PG-M1) or CD68 (KP1) labeled pure epithelioid PEComa /epithelioid angiomyolipomas. On the other hand, all MiT family translocation renal cell carcinomas were completely negative for CD68 (PG-M1) but positive for CD68 (KP1), supporting the usefulness of CD68 (PG-M1) along with PAX8 in distinguishing MiT family translocation renal cell carcinoma from pure epithelioid PEComa /epithelioid angiomyolipoma. The absence of CD68 (PG-M1) was surprising in that *TFEB/TFE3* are known to be master regulators of lysosomal

proteins expression, and it thought to drive expression of cathepsin K in the MiT family translocation renal cell carcinoma. A possible explanation could be attributed to the different epitopes recognized by the two different clones; the epitope recognized by CD68 (PG-M1) might be lost or masked during carcinogenesis.

Another important aspect of this study is the proper cut-off to define the occurrence of *TFEB* rearrangement in t(6;11) renal cell carcinoma and *TFE3* rearrangement in Xp11 renal cell carcinoma. Using standard criteria determined by scoring normal tissues for clinical assays, Argani et al. [20] defined a positive FISH result in their clinical assay as when the fluorescent signals were separated by a signal diameter >1 in at least 15.8% neoplastic cells using standardized published methodology. In this study, we observed a high frequency (74% and 68%) of split signals ($\geq$ 2 signals diameter) in t(6;11) renal cell carcinomas and Xp11 renal cell carcinomas, ranging from 61% to 94% and from 45% to 94%. Similar results have been published by Smith et al., reporting high frequency of split signals (range from 38% to 86%, mean 69%) in 10 cases of t(6;11) renal cell carcinoma [21].

With regards to t(6;11) renal cell carcinoma, it is known that most instances have an indolent clinical course with a few published cases demonstrating aggressive behavior [14, 20, 21, 26, 29-32]. In this study, we reported 2 patients with t(6;11) renal cell carcinoma who both developed metastasis after 24 months. In both cases, we histologically confirmed the metastasis and FISH assay was performed in primary and metastatic samples. In our review of the literature, we have identified nine t(6;11) renal cell carcinomas with aggressive behavior. Among them, in 2 tumors no molecular analysis for the presence of translocation (6;11) was carried out [14, 29], in the remaining karyotyping or FISH assay have revealed *TFEB* rearrangement. However, the recurrences have been usually reported as only a clinical finding. In only one case, lung metastasis was histologically examined and the presence of t(6;11)(p21.1;q12~13) chromosomal rearrangement was demonstrated; that patient had a renal tumor diagnosed as "clear cell renal cell carcinoma" 8 years before which was not reevaluated for the presence of translocation [30]. Interestingly, we also reported an increasing number

of TFEB fluorescent signals (3-5 signals) in the two aggressive cases of our series. This drew our attention since *TFEB* amplified renal cell carcinoma has been recently described [26, 27, 49]. Hence, we investigated the possibility of *TFEB* amplification and FISH analysis with a chromosome 6 centromeric probe. After the correction by chromosome 6 centromeric probe, we observed a similar increased number of TFEB and CEP6 fluorescent signals; therefore, we did not consider them as amplified tumors. Nevertheless, the occurrence of *TFEB* gene copy number gains is particularly interesting since both *TFEB* amplification and rearrangement have been demonstrated in two previously published primary tumors[26, 31]. It is worth noting that Peckova et al. reported the presence of amplification without any additional details whereas Argani et al. defined amplification as >10:1 ratio of TFEB fluorescent signal to centromeric probe. This aspect is fascinating because it is possible that increasing in copy number of *TFEB* gene region in t(6;11) renal cell carcinoma may predict an aggressive clinical course. In this light, we may speculate that the occurrence of *TFEB* gene copy number gains in our two aggressive cases might be the result of genomic instability. However, further investigations of larger series should be conducted to validate this result.

Overall, t(6;11) renal cell carcinomas described in this article occurred in patients around 40 years, the tumors' size was 7.5 cm without a typical gross appearance (6 of 7 tumors were solid and one tumor extensively cystic). Interestingly, one patient (case 5) was previously treated with chemotherapy for the diagnosis of non Hodgkin lymphoma. However, the occurrence of t(6;11) renal cell carcinoma associated to a history of prior exposure to chemotherapy is known[9]. The characteristic biphasic morphology due to the presence of larger epithelioid cells and smaller cells surrounding basement membrane material was noted in 1 of 7 tumors (case 3). A discontinuous pseudocapsule was present in 5 of 7 tumors and psammoma bodies were encountered in half tumors. Bony metaplasia and hyalinized stroma with thick-walled vessels were observed in two tumors. The cells typically showed nucleolar grade G2 and G3 by ISUP/WHO 2016. Tumor necrosis was absent and the proliferation rate was low with the

exception of the two aggressive tumors in which focal necrosis and mitotic activity were found.

With respect to aggressive t(6;11) renal cell carcinoma, the present series as well as the review of the literature provides some useful information. Renal cell carcinoma with *TFEB* rearrangement displayed an aggressive behavior in roughly 17% of cases (11 of 64), occurring as larger masses (12 versus 7 cm) in older patients (46 versus 30 years). It should be noted that hematogenous metastasis are more common than nodal metastasis, which was reported in two cases without molecular confirmation of t(6;11) rearrangement.

An increasing number of manuscripts reported the presence of *TFEB* gene amplification in renal cell carcinoma [26, 27, 50-52]. Since this tumor is defined by the occurrence of *TFEB* gene amplification what is considered amplified is of paramount importance. Gene amplification is established as an elevated extra copies of a gene without a proportional increase in other genes. Generally speaking, amplification of a gene may have diagnostic value (e.g. *MDM2* amplification in well-differentiated liposarcoma) [53], prognostic value (e.g. *MYC* amplification in neuroblastoma) [54] or predictive value (e.g. *HER-2* amplification in breast carcinoma)[55]. In renal cell carcinoma, *TFEB* gene amplification seems to be correlated with an aggressive behavior. The threshold proposed by Argani and coauthors is defined by the presence of an average of 10 or more copies per neoplastic nucleus [26]. Given the lack of a consensus to define *TFEB* amplification, Gupta et al. arbitrarily defined two levels of amplification, a low-level characterized by 5-10 copies and an high-level with >10 copies [27]. Since the other studies used a cut-off of >10 copies per nuclei, we decided to consider the latter as the threshold to use. Moreover, in previous analysis [26, 27, 50, 52], no percentage of tumor cells harboring the amplification has been recorded, except in one recent study in which at least 10% of cells demonstrated the increasing fluorescent signals to consider the case amplified [51]. In the present series, the 3 tumors with *TFEB* amplification showed an increased gene copy number in virtually all neoplastic nuclei.

Another open and controversial issue is whether the increase of *TFEB* gene copy number is due to nonspecific whole DNA polyploidy versus locus

specific *TFEB* amplification, in other words, whether it is a specific or nonspecific event. After corrections for centromeric alpha-satellite specific for chromosome 6, *TFEB* gene copy number was interpreted as true amplification rather than an nonspecific polyploidy in three cases (case 30, case 31 and case 32). On the other hand, two cases (case 28 and case 29) showed a lower level of gene copy number (3-5 signals per tumor nuclei) with a similar increased number of CEP6. Hence, these were considered as chromosome 6 polysomy, a nonspecific event reflecting genomic instability.

Because of its novelty, the characteristics of TFEB-amplified renal cell carcinoma are not well understood; therefore, we undertook a comprehensive review of this tumor as illustrated in Table 10. Overall, 42 cases of TFEB-amplified renal cell carcinoma, including the 3 cases described herein, with or without *TFEB* rearrangement were found. The mean age of these patients was 63 years and the median 65 years (range from 23 to 83). There was a slight male predominance (24M, 18F). The tumors' size ranged from 1.8 to 19.5 cm (mean and median 10). When follow up was available, it ranged from 1 to 265 months (mean 79 and median 24). Based upon the review of the literature, the majority (26/41, 63%) of TFEB-amplified renal cell carcinomas are tumor stage pT3 or higher which correlates with the aggressiveness. Moreover, most of the tumors (88%) showed an high ISUP/WHO 2016 nucleolar grade. Interestingly, as previously noted [27, 56] and here reported, *TFEB* amplification may occur in low grade renal cell carcinoma. Histologically, the tumors with *TFEB* amplification were mainly characterized by a nested or papillary/psuedopapillary architecture made up of epithelioid cells with eosinophilic cytoplasm. None of the four t(6;11) renal cell carcinomas with concurrent *TFEB* gene amplification demonstrated the classical biphasic morphology with larger epithelioid cells and smaller cells clustered around eosinophilic spheres formed by basement membrane material. Nevertheless, the amplified - t(6;11) renal cell carcinoma (case 30) described in the present study showed two types of cells, large and small size. Immunohistochemically, labeling for HMB45, when reported present (6/27, 22%), is usually focal whereas the positivity of cathepsin K (14/21, 67%) and Melan-A (26/33, 79%) ranged from patchy to diffuse. Among the four cases of t(6;11) renal

cell carcinoma with concurrent *TFEB* gene amplification, all tumors expressed Melan-A, cathepsin K was present in 3 of 4, and half of them were labeled by HMB45. The expression of cathepsin K and melanocytic markers in TFEB-amplified renal cell carcinoma is worthy of note. A possible explanation is that, not only *TFEB* rearrangement but also increased *TFEB* gene copy number leads to intact TFEB protein overexpression which correlates with aberrant melanocytic marker immunolabeling and cathepsin K expression as well.

In the current study, we have also assessed the occurrence of *VEGFA* amplification in renal cell carcinomas with *TFEB* gene alterations, either amplification or rearrangement. Increased *VEGFA* gene copy number (3-5 signals) was found in the two aggressive cases of t(6;11) renal cell carcinoma with a similar number of TFEB fluorescent signals. In the three TFEB-amplified renal cell carcinomas (>10 TFEB signals), a concurrent *VEGFA* amplification was observed. The mRNA expression of VEGFA analyzed by RNAscope was concordant with *VEGFA* status in 7 out of 10 tumors (5 VEGFA mRNA positive cases with VEGFA and TFEB gene copy number/amplification and 2 VEGFA mRNA negative cases with VEGFA and TFEB disomic status). In the remaining three cases, the level of VEGFA mRNA was higher than expected based on the level of *VEGFA* gene copy number suggesting the involvement of an alternative mechanism leading the upregulation of mRNA expression.

We have also analyzed 22 cases of Xp11 renal cell carcinoma. In the present series, Xp11 renal cell carcinoma occurred in patients around 40 years with almost equal prevalence in both sexes. Four patients (n. 4, 9, 13 16) were at advanced stage at the diagnosis with lymph node metastasis. One patient (n. 7) developed multiple peritoneal metastasis sixty months after the surgery. Regarding histology the tumors presented a wide spectrum of architectures and morphologies, as previously reported[3]. Interestingly three cases showed an almost identical growth pattern characterized by multiple cysts lined by medium sized cells with clear cytoplasm and G2 nuclear grade sec. WHO/ISUP 2016.

These tumors shared an identical immunophenotype being diffusely positive for cathepsin K, Melan-A and negative for HMB45. It is of interest that those tumors were the only cases positive for Melan-A while all the others Xp11 renal cell

carcinomas were negative. Cases of extensively cystic Xp11 renal cell carcinoma have been recently described by Wang and colleagues[57]. In those tumors the *TFE3* gene was fused with the gene *MED15*, so it is possible to speculate that also the three cystic tumors herein reported are characterized by the same novel gene fusion.

The last fascinating aspect regards the treatment. At present, there are few studies concerning the target therapy (mTOR inhibitor and anti-angiogenic including anti-VEGF receptor and ligand) in MiT family translocation renal cell carcinoma [15, 16]. It is important to note that all the tumors of the patients reported by Malouf et al. and Choueiri et al. were Xp11 renal cell carcinoma and data regarding the treatment of aggressive t(6;11) renal cell carcinoma are lacking. Recently, Gupta and colleagues described the possible usefulness of VEGFR target therapy in four renal cell carcinomas with TFEB/VEGFA coamplification [27]. This finding is interesting since the t(6;11) renal cell carcinoma with aggressive behavior reported in the present study were characterized by increased TFEB/VEGFA gene copy number suggesting that VEGFA may be a potential therapeutic target in this subset of tumors. Moreover, a tyrosine kinase inhibitor with activity against VEGF, MET, and AXL has been recently proposed in the treatment of advanced renal cell carcinomas. It has been demonstrated in vitro the inhibition of the osteoclast differentiation, down-regulating several molecules such as cathepsin K, after non-cytotoxic doses of this treatment [58, 59]. Some medical trials conducted on conventional renal cell carcinomas have shown that this drug could be highly effective in inducing tumor regression even in cases where antiangiogenetic drugs and m-TOR inhibitors have failed [18, 60-62].

MET is a membrane receptor sensitive to hepatocyte growth factor and that activates an intracellular signalling pathway very important in the renal physiology. The hepatocyte growth factor in the kidney stimulates tissue regeneration following an insult, promotes the production of molecules with anti-oxidant, anti-inflammatory functions and that inhibit fibrogenesis. In the cell it stimulates mitosis, migration and has antiapoptotic effects; therefore an unregulated activation of MET can promote oncogenesis and support tumor growth. It has been shown that TFE3 can be a strong promoter of MET

transcription and that the pathway of liver growth factor is important in the oncogenesis of tumors that have an over expression of TFE3 [18]. On the other hand, AXL is a tyrosine kinase receptor belonging to the subfamily of TAM receptors. It acts as a GAS6 receptor, a factor that stimulates cell growth. The signaling pathway activated by AXL promotes numerous cellular processes including proliferation, adhesion, migration and therefore AXL can act a pro-oncogenic potential [63].

Based upon the possibility to use a tyrosine kinase inhibitor with activity against VEGF, MET, and AXL we analyzed the immunohistochemical expression of MET and AXL in MiT family translocation renal cell carcinoma. The expression of these molecules in the tumor samples would provide an evidence to support the use of this drug in those cases. In the present study, none cases showed AXL positivity, whereas 61% of Xp11 renal cell carcinomas and 70% of t(6;11) renal cell carcinomas were labeled for MET.

In summary, in this study we present the clinical, morphological and molecular features of a large series of MiT family translocation renal cell carcinoma and TFEB-amplified renal cell carcinoma. We report the high frequency of split signals by FISH in MiT family translocation renal cell carcinomas and the occurrence of gene copy number increases in the aggressive cases. We demonstrate the usefulness of CD68 (PG-M1) immunohistochemical staining in distinguishing MiT family translocation renal cell carcinoma from pure epithelioid PEComa /epithelioid angiomyolipoma. Finally, we suggest VEGF and MET as potential therapeutic target in aggressive MiT family translocation renal cell carcinomas

Table 10. Renal cell carcinomas with TFEB amplification

Case	References	Age	Gender	Size (cm)	Stage TNM	ISUP grade	PAX2/PAX8	Cathepsin K	HMB45	Melan-A	TFEB FISH	VEGFA FISH	Follow up	Notes
1	Peckova et al, 2014	77	F	12	pT3NxM1	4	+	+	+	+	break + amplification*	NA	dead after 2,5 months	adrenal gland and lung metastasis
2	Durinck et al, 2014	56	M	NA	NA	low	NA	NA	NA	NA	NA	NA	NA	
3	Argani et al, 2016	64	F	10.9	pT3bN2Mx	3	+	neg	neg	+	>10 signals	NA	28 months alive	renal vein thrombus
4	Argani et al, 2016	71	M	3	pT3aNxMx	3	+	neg	neg	+	>10 signals	NA		periaortic lymph node metastasis
5	Argani et al, 2016	65	M	1.9	pT1NxMx	3	+	+	neg	+	>10 signals	NA	NA	
6	Argani et al, 2016	23	F	7	pT2NxMx	4	+	+	+	+	>10 signals	NA		vaginal metastasis
7	Argani et al, 2016	77	F	4	pT1NxMx	3	+	+	+	+	>10 signals	NA	NA	
8	Argani et al, 2016	78	F	12	pT3bNxMx	3	+	+	neg	+	>10 signals	NA	NA	renal vein thrombus
9	Argani et al, 2016	61	F	19	pT4N0M1	4	+	neg	neg	+	break + >10 signals	NA	NA	vaginal metastasis
10	Argani et al, 2016	61	M	2.7	pT1NxMx	3	+	+	+	+	break + >10 signals	NA	NA	
11	Williamson et al, 2016	57	M	19.5	pT3aN0Mx	NA	+	+	NA	+	>10 signals	NA	NA	
12	Williamson et al, 2016	62	F	12.5	pT3aNxMx	NA	NA	neg	neg	neg	>10 signals	NA	NA	
13	Williamson et al, 2016	78	F	4.3	pT3aNxMx	NA	NA	+	NA	+	>10 signals	NA	NA	
14	Williamson et al, 2016°	64	M	11	pT3aN0Mx	NA	NA	NA	NA	NA	>10 signals	NA	NA	
15	Williamson et al, 2016°	59	M	9.2	pT2aN1Mx	NA	NA	NA	NA	NA	>10 signals	NA	NA	
16	Williamson et al, 2016°	71	M	8	pT3aNxMx	NA	NA	NA	NA	NA	>10 signals	NA	NA	
17	Williamson et al, 2016°	28	F	6.5	pT3aN1Mx	NA	+	NA	NA	NA	>10 signals	NA	NA	
18	Williamson et al, 2016°	61	F	5.3	pT3aNxMx	NA	NA	NA	NA	NA	>10 signals	NA	NA	
19	Williamson et al, 2016°	59	M	4.5	pT1bNxMx	NA	NA	NA	NA	NA	>10 signals	NA	NA	
20	Gupta et al, 2017	34	M	9	pT3cNxM1	3	NA	NA	neg	+	>10 signals	>10 signals	dead after 21 months	soft tissue metastasis
21	Gupta et al, 2017	80	M	1.8	pT1aNxM0	3	NA	NA	neg	neg	>10 signals	>10 signals	dead after 47 months	
22	Gupta et al, 2017	65	F	9.5	pT3aNxM0	3	NA	NA	neg	neg	>10 signals	>10 signals	dead after 73 months	soft tissue metastasis
23	Gupta et al, 2017	69	F	2.5	pT1aNxM0	2	NA	NA	neg	+	>10 signals	>10 signals	265 months alive	
24	Gupta et al, 2017	78	M	5.5	pT3cNxM0	3	NA	NA	neg	+	>10 signals	>10 signals	dead after 254 months	
25	Gupta et al, 2017	62	M	13	pT2bNxM0	2	NA	NA	+	+	>10 signals	>10 signals	dead after 194 months	
26	Gupta et al, 2017	70	M	10	pT2aN1M0	4	NA	NA	neg	+	>10 signals	>10 signals	dead after 18 months	bone and lung metastasis

27	Gupta et al, 2017	83	M	6.5	pT3cNxM1	4	NA	NA	neg	+	>10 signals	>10 signals	dead after 40 months	brain, lung, adrenal gland and lymph nodes
28	Gupta et al, 2017	56	M	13	pT3aNxM0	4	NA	NA	neg	neg	>10 signals	5 signals	dead after 242 months	
29	Gupta et al, 2017	73	M	3.7	pT3aNxMx	3	+	+	NA	NA	>10 signals	NA	NA	
30	Gupta et al, 2017	68	F	18.5	pT3cN0Mx	3	NA	NA	neg	+	>10 signals	>10 signals	dead after 18 months	bone and soft tissue metastasis
31	Skala et al, 2017	68	F	6.5	pT3aNxMx	3	NA	+	NA	+	>10 signals	NA	NA	
32	Skala et al, 2017	65	M	5.5	pT3aNxMx	3	NA	+	NA	NA	>10 signals	NA	NA	
33	Skala et al, 2017	48	F	10.1	pT2bNxMx	4	NA	NA	NA	+	>10 signals	NA	NA	
34	Skala et al, 2017	68	M	12.2	pT4N1M1	4	+	NA	neg	+	>10 signals	NA	NA	
35	Skala et al, 2017	72	M	7	pT3aNxMx	3	+	NA	NA	+	>10 signals	NA	NA	
36	Skala et al, 2017	69	M	5.9	pT3aN1Mx	3	NA	NA	NA	+	>10 signals	NA	NA	
37	Mendel et.al, 2017	55	F	8	pT2aN0M0	4	NA	neg	neg	neg	>20 signals	NA (array CGH)	161 moths alive	lung metastasis
38	Mendel et.al, 2017	55	F	17	pT4NxM1	4	NA	neg	neg	neg	4-10 signals	NA (array CGH)	dead after 1 month	renal vein thrombus, brain metastasis
39	Mendel et.al, 2017	60	M	14	pT3cN0M1	4	NA	neg	neg	+ (40%)	10-20 signals	NA (array CGH)	dead after 14 months	renal vein thrombus, liver metastasis
40	Present series (case 30)	69	M	7	pT2aNxMx	3	+ (30%)	+ (40%)	neg	+ (90%)	break + >10 signals	> 10 signals	14 months alive	perinephric nodules after 5 months
41	Present series (case 31)	41	F	3	pT1aNxMx	2	+ (50%)	+ (100%)	+ (1%)	+ (5%)	>10 signals	> 10 signals (10% of nuclei) 6 signals (90% of nuclei)	20 months alive	
42	Present series (case 32)	79	M	10	pT2aNxMx	3	+ (50%)	+ (10%)	neg	neg	>10 signals	> 10 signals (80% of nuclei) 6 signals (20% of nuclei)	18 months alive	
NA: not available, * no additional information, ° cases from TCGA														

REFERENCES

1. Haq R, Fisher DE. Biology and clinical relevance of the micropthalmia family of transcription factors in human cancer. *J Clin Oncol*. 2011;**29**:3474-82.
2. Moch H, Humprey PA, Ulbright TM, Reuter VE. WHO Classification of Tumours of the Urinary System and Male Genital Organs. Cancer IAfRo, editor. Lyon, France 2016.
3. Argani P. MiT family translocation renal cell carcinoma. *Semin Diagn Pathol*. 2015;**32**:103-13.
4. Xia QY, Wang XT, Ye SB, Wang X, Li R, Shi SS, et al. Novel gene fusion of PRCC-MITF defines a new member of MiT family translocation renal cell carcinoma: clinicopathological analysis and detection of the gene fusion by RNA sequencing and FISH. *Histopathology*. 2018;**72**:786-94.
5. Xia QY, Wang XT, Zhan XM, Tan X, Chen H, Liu Y, et al. Xp11 Translocation Renal Cell Carcinomas (RCCs) With RBM10-TFE3 Gene Fusion Demonstrating Melanotic Features and Overlapping Morphology With t(6;11) RCC: Interest and Diagnostic Pitfall in Detecting a Paracentric Inversion of TFE3. *Am J Surg Pathol*. 2017;**41**:663-76.
6. Xia QY, Wang Z, Chen N, Gan HL, Teng XD, Shi SS, et al. Xp11.2 translocation renal cell carcinoma with NONO-TFE3 gene fusion: morphology, prognosis, and potential pitfall in detecting TFE3 gene rearrangement. *Mod Pathol*. 2017;**30**:416-26.
7. Argani P, Antonescu CR, Illei PB, Lui MY, Timmons CF, Newbury R, et al. Primary renal neoplasms with the ASPL-TFE3 gene fusion of alveolar soft part sarcoma: a distinctive tumor entity previously included among renal cell carcinomas of children and adolescents. *Am J Pathol*. 2001;**159**:179-92.
8. Sukov WR, Hodge JC, Lohse CM, Leibovich BC, Thompson RH, Pearce KE, et al. TFE3 rearrangements in adult renal cell carcinoma: clinical and pathologic features with outcome in a large series of consecutively treated patients. *Am J Surg Pathol*. 2012;**36**:663-70.
9. Argani P, Lae M, Ballard ET, Amin M, Manivel C, Hutchinson B, et al. Translocation carcinomas of the kidney after chemotherapy in childhood. *J Clin Oncol*. 2006;**24**:1529-34.
10. Argani P, Hicks J, De Marzo AM, Albadine R, Illei PB, Ladanyi M, et al. Xp11 translocation renal cell carcinoma (RCC): extended immunohistochemical profile emphasizing novel RCC markers. *Am J Surg Pathol*. 2010;**34**:1295-303.
11. Martignoni G, Gobbo S, Camparo P, Brunelli M, Munari E, Segala D, et al. Differential expression of cathepsin K in neoplasms harboring TFE3 gene fusions. *Mod Pathol*. 2011;**24**:1313-9.
12. Green WM, Yonescu R, Morsberger L, Morris K, Netto GJ, Epstein JI, et al. Utilization of a TFE3 break-apart FISH assay in a renal tumor consultation service. *Am J Surg Pathol*. 2013;**37**:1150-63.
13. Ellis CL, Eble JN, Subhawong AP, Martignoni G, Zhong M, Ladanyi M, et al. Clinical heterogeneity of Xp11 translocation renal cell carcinoma: impact of fusion subtype, age, and stage. *Mod Pathol*. 2014;**27**:875-86.
14. Camparo P, Vasiliu V, Molinie V, Couturier J, Dykema KJ, Petillo D, et al. Renal translocation carcinomas: clinicopathologic, immunohistochemical, and

gene expression profiling analysis of 31 cases with a review of the literature. *Am J Surg Pathol*. 2008;**32**:656-70.
15. Choueiri TK, Lim ZD, Hirsch MS, Tamboli P, Jonasch E, McDermott DF, et al. Vascular endothelial growth factor-targeted therapy for the treatment of adult metastatic Xp11.2 translocation renal cell carcinoma. *Cancer*. 2010;**116**:5219-25.
16. Malouf GG, Camparo P, Oudard S, Schleiermacher G, Theodore C, Rustine A, et al. Targeted agents in metastatic Xp11 translocation/TFE3 gene fusion renal cell carcinoma (RCC): a report from the Juvenile RCC Network. *Ann Oncol*. 2010;**21**:1834-8.
17. Chang K, Qu Y, Dai B, Zhao JY, Gan H, Shi G, et al. PD-L1 expression in Xp11.2 translocation renal cell carcinoma: Indicator of tumor aggressiveness. *Sci Rep*. 2017;**7**:2074.
18. Tsuda M, Davis IJ, Argani P, Shukla N, McGill GG, Nagai M, et al. TFE3 fusions activate MET signaling by transcriptional up-regulation, defining another class of tumors as candidates for therapeutic MET inhibition. *Cancer Res*. 2007;**67**:919-29.
19. Argani P, Hawkins A, Griffin CA, Goldstein JD, Haas M, Beckwith JB, et al. A distinctive pediatric renal neoplasm characterized by epithelioid morphology, basement membrane production, focal HMB45 immunoreactivity, and t(6;11)(p21.1;q12) chromosome translocation. *Am J Pathol*. 2001;**158**:2089-96.
20. Argani P, Yonescu R, Morsberger L, Morris K, Netto GJ, Smith N, et al. Molecular confirmation of t(6;11)(p21;q12) renal cell carcinoma in archival paraffin-embedded material using a break-apart TFEB FISH assay expands its clinicopathologic spectrum. *Am J Surg Pathol*. 2012;**36**:1516-26.
21. Smith NE, Illei PB, Allaf M, Gonzalez N, Morris K, Hicks J, et al. t(6;11) renal cell carcinoma (RCC): expanded immunohistochemical profile emphasizing novel RCC markers and report of 10 new genetically confirmed cases. *Am J Surg Pathol*. 2014;**38**:604-14.
22. Rao Q, Zhang XM, Tu P, Xia QY, Shen Q, Zhou XJ, et al. Renal cell carcinomas with t(6;11)(p21;q12) presenting with tubulocystic renal cell carcinoma-like features. *Int J Clin Exp Pathol*. 2013;**6**:1452-7.
23. Martignoni G, Pea M, Gobbo S, Brunelli M, Bonetti F, Segala D, et al. Cathepsin-K immunoreactivity distinguishes MiTF/TFE family renal translocation carcinomas from other renal carcinomas. *Mod Pathol*. 2009;**22**:1016-22.
24. Martignoni G, Bonetti F, Chilosi M, Brunelli M, Segala D, Amin MB, et al. Cathepsin K expression in the spectrum of perivascular epithelioid cell (PEC) lesions of the kidney. *Mod Pathol*. 2012;**25**:100-11.
25. Argani P, Lae M, Hutchinson B, Reuter VE, Collins MH, Perentesis J, et al. Renal carcinomas with the t(6;11)(p21;q12): clinicopathologic features and demonstration of the specific alpha-TFEB gene fusion by immunohistochemistry, RT-PCR, and DNA PCR. *Am J Surg Pathol*. 2005;**29**:230-40.
26. Argani P, Reuter VE, Zhang L, Sung YS, Ning Y, Epstein JI, et al. TFEB-amplified Renal Cell Carcinomas: An Aggressive Molecular Subset Demonstrating Variable Melanocytic Marker Expression and Morphologic Heterogeneity. *Am J Surg Pathol*. 2016;**40**:1484-95.

27. Gupta S, Johnson SH, Vasmatzis G, Porath B, Rustin JG, Rao P, et al. TFEB-VEGFA (6p21.1) co-amplified renal cell carcinoma: a distinct entity with potential implications for clinical management. *Mod Pathol*. 2017;**30**:998-1012.
28. Pecciarini L, Cangi MG, Lo Cunsolo C, Macri E, Dal Cin E, Martignoni G, et al. Characterization of t(6;11)(p21;q12) in a renal-cell carcinoma of an adult patient. *Genes Chromosomes Cancer*. 2007;**46**:419-26.
29. Ishihara A, Yamashita Y, Takamori H, Kuroda N. Renal carcinoma with (6;11)(p21;q12) translocation: report of an adult case. *Pathol Int*. 2011;**61**:539-45.
30. Inamura K, Fujiwara M, Togashi Y, Nomura K, Mukai H, Fujii Y, et al. Diverse fusion patterns and heterogeneous clinicopathologic features of renal cell carcinoma with t(6;11) translocation. *Am J Surg Pathol*. 2012;**36**:35-42.
31. Peckova K, Vanecek T, Martinek P, Spagnolo D, Kuroda N, Brunelli M, et al. Aggressive and nonaggressive translocation t(6;11) renal cell carcinoma: comparative study of 6 cases and review of the literature. *Ann Diagn Pathol*. 2014;**18**:351-7.
32. Lilleby W, Vlatkovic L, Meza-Zepeda LA, Revheim ME, Hovig E. Translocational renal cell carcinoma (t(6;11)(p21;q12) with transcription factor EB (TFEB) amplification and an integrated precision approach: a case report. *J Med Case Rep*. 2015;**9**:281.
33. Davis IJ, Hsi BL, Arroyo JD, Vargas SO, Yeh YA, Motyckova G, et al. Cloning of an Alpha-TFEB fusion in renal tumors harboring the t(6;11)(p21;q13) chromosome translocation. *Proc Natl Acad Sci U S A*. 2003;**100**:6051-6.
34. Argani P, Ladanyi M. Translocation carcinomas of the kidney. *Clin Lab Med*. 2005;**25**:363-78.
35. Kuiper RP, Schepens M, Thijssen J, van Asseldonk M, van den Berg E, Bridge J, et al. Upregulation of the transcription factor TFEB in t(6;11)(p21;q13)-positive renal cell carcinomas due to promoter substitution. *Hum Mol Genet*. 2003;**12**:1661-9.
36. Geller JI, Argani P, Adeniran A, Hampton E, De Marzo A, Hicks J, et al. Translocation renal cell carcinoma: lack of negative impact due to lymph node spread. *Cancer*. 2008;**112**:1607-16.
37. Hora M, Hes O, Urge T, Eret V, Klecka J, Michal M. A distinctive translocation carcinoma of the kidney ["rosette-like forming," t(6;11), HMB45-positive renal tumor]. *Int Urol Nephrol*. 2009;**41**:553-7.
38. Petersson F, Vanecek T, Michal M, Martignoni G, Brunelli M, Halbhuber Z, et al. A distinctive translocation carcinoma of the kidney; "rosette forming," t(6;11), HMB45-positive renal tumor: a histomorphologic, immunohistochemical, ultrastructural, and molecular genetic study of 4 cases. *Hum Pathol*. 2012;**43**:726-36.
39. Zhan HQ, Wang CF, Zhu XZ, Xu XL. Renal cell carcinoma with t(6;11) translocation: a patient case with a novel Alpha-TFEB fusion point. *J Clin Oncol*. 2010;**28**:e709-13.
40. Malouf GG, Camparo P, Molinie V, Dedet G, Oudard S, Schleiermacher G, et al. Transcription factor E3 and transcription factor EB renal cell carcinomas: clinical features, biological behavior and prognostic factors. *J Urol*. 2011;**185**:24-9.
41. Suarez-Vilela D, Izquierdo-Garcia F, Mendez-Alvarez JR, Miguelez-Garcia E, Dominguez-Iglesias F. Renal translocation carcinoma with expression

of TFEB: presentation of a case with distinctive histological and immunohistochemical features. *Int J Surg Pathol*. 2011;**19**:506-9.
42. Rao Q, Liu B, Cheng L, Zhu Y, Shi QL, Wu B, et al. Renal cell carcinomas with t(6;11)(p21;q12): A clinicopathologic study emphasizing unusual morphology, novel alpha-TFEB gene fusion point, immunobiomarkers, and ultrastructural features, as well as detection of the gene fusion by fluorescence in situ hybridization. *Am J Surg Pathol*. 2012;**36**:1327-38.
43. Zhong M, De Angelo P, Osborne L, Paniz-Mondolfi AE, Geller M, Yang Y, et al. Translocation renal cell carcinomas in adults: a single-institution experience. *Am J Surg Pathol*. 2012;**36**:654-62.
44. Matsuura K, Inoue T, Kai T, Yano S, Kashima K, Yokoyama S, et al. Molecular analysis of a case of renal cell carcinoma with t(6;11)(p21;q12) reveals a link to a lysosome-like structure. *Histopathology*. 2014;**64**:306-9.
45. Arneja SK, Gujar N. Renal cell carcinoma with t(6:11) (p21;q12). A case report highlighting distinctive immunohistologic features of this rare tumor. *Int J Surg Case Rep*. 2015;**7C**:16-9.
46. Wolff N, Kabbani W, Bradley T, Raj G, Watumull L, Brugarolas J. Sirolimus and temsirolimus for epithelioid angiomyolipoma. *J Clin Oncol*. 2010;**28**:e65-8.
47. Williamson SR, Eble JN, Palanisamy N. Sclerosing TFEB-rearrangement renal cell carcinoma: a recurring histologic pattern. *Hum Pathol*. 2017;**62**:175-79.
48. Martignoni G, Pea M, Zampini C, Brunelli M, Segala D, Zamboni G, et al. PEComas of the kidney and of the genitourinary tract. *Semin Diagn Pathol*. 2015;**32**:140-59.
49. Williamson SR, Grignon DJ, Cheng L, Favazza L, Gondim DD, Carskadon S, et al. Renal Cell Carcinoma With Chromosome 6p Amplification Including the TFEB Gene: A Novel Mechanism of Tumor Pathogenesis? *Am J Surg Pathol*. 2016.
50. Williamson SR, Grignon DJ, Cheng L, Favazza L, Gondim DD, Carskadon S, et al. Renal Cell Carcinoma With Chromosome 6p Amplification Including the TFEB Gene: A Novel Mechanism of Tumor Pathogenesis? *Am J Surg Pathol*. 2017;**41**:287-98.
51. Mendel L, Ambrosetti D, Bodokh Y, Ngo-Mai M, Durand M, Simbsler-Michel C, et al. Comprehensive study of three novel cases of TFEB-amplified renal cell carcinoma and review of the literature: Evidence for a specific entity with poor outcome. *Genes Chromosomes Cancer*. 2018;**57**:99-113.
52. Skala SL, Xiao H, Udager AM, Dhanasekaran SM, Shukla S, Zhang Y, et al. Detection of 6 TFEB-amplified renal cell carcinomas and 25 renal cell carcinomas with MITF translocations: systematic morphologic analysis of 85 cases evaluated by clinical TFE3 and TFEB FISH assays. *Mod Pathol*. 2018;**31**:179-97.
53. Zhang H, Erickson-Johnson M, Wang X, Oliveira JL, Nascimento AG, Sim FH, et al. Molecular testing for lipomatous tumors: critical analysis and test recommendations based on the analysis of 405 extremity-based tumors. *Am J Surg Pathol*. 2010;**34**:1304-11.
54. Canete A, Gerrard M, Rubie H, Castel V, Di Cataldo A, Munzer C, et al. Poor survival for infants with MYCN-amplified metastatic neuroblastoma despite

intensified treatment: the International Society of Paediatric Oncology European Neuroblastoma Experience. *J Clin Oncol*. 2009;**27**:1014-9.
55. Slamon DJ, Leyland-Jones B, Shak S, Fuchs H, Paton V, Bajamonde A, et al. Use of chemotherapy plus a monoclonal antibody against HER2 for metastatic breast cancer that overexpresses HER2. *N Engl J Med*. 2001;**344**:783-92.
56. Durinck S, Stawiski EW, Pavia-Jimenez A, Modrusan Z, Kapur P, Jaiswal BS, et al. Spectrum of diverse genomic alterations define non-clear cell renal carcinoma subtypes. *Nat Genet*. 2015;**47**:13-21.
57. Wang XT, Xia QY, Ye SB, Wang X, Li R, Fang R, et al. RNA sequencing of Xp11 translocation-associated cancers reveals novel gene fusions and distinctive clinicopathologic correlations. *Mod Pathol*. 2018;**31**:1346-60.
58. Grullich C. Cabozantinib: Multi-kinase Inhibitor of MET, AXL, RET, and VEGFR2. *Recent Results Cancer Res*. 2018;**211**:67-75.
59. Markowitz JN, Fancher KM. Cabozantinib: A Multitargeted Oral Tyrosine Kinase Inhibitor. *Pharmacotherapy*. 2018;**38**:357-69.
60. Bersanelli M, Buti S. Cabozantinib in metastatic renal cell carcinoma: latest findings and clinical potential. *Ther Adv Med Oncol*. 2017;**9**:627-36.
61. Choueiri TK, Escudier B, Powles T, Tannir NM, Mainwaring PN, Rini BI, et al. Cabozantinib versus everolimus in advanced renal cell carcinoma (METEOR): final results from a randomised, open-label, phase 3 trial. *Lancet Oncol*. 2016;**17**:917-27.
62. Choueiri TK, Halabi S, Sanford BL, Hahn O, Michaelson MD, Walsh MK, et al. Cabozantinib Versus Sunitinib As Initial Targeted Therapy for Patients With Metastatic Renal Cell Carcinoma of Poor or Intermediate Risk: The Alliance A031203 CABOSUN Trial. *J Clin Oncol*. 2017;**35**:591-97.
63. Wu X, Liu X, Koul S, Lee CY, Zhang Z, Halmos B. AXL kinase as a novel target for cancer therapy. *Oncotarget*. 2014;**5**:9546-63.